IJE TRANSACTIONS B: Applications Vol. 38 No. 05, (May 2025) 1190-1212

International Journal of Engineering

Journal Homepage: www.ije.ir

Predictive Model of Bond Strength in Reinforced Concrete Structures: A Hybrid Metaheuristic-optimized Neural Network Approach

N. Safaeian Hamzehkolaei*[a], S. Ghavaminejad[b], M. S. Barkhordari[c]

[a] *Department of Civil Engineering, Bozorgmehr University of Qaenat, Qaen, Iran*
[b] *Faculty of Engineering, Pardis Science and Technology Branch, Islamic Azad University, Pardis, Iran*
[c] *Department of Civil Engineering, Amirkabir University of Technology (Tehran Polytechnic), Tehran, Iran*

P A P E R I N F O

Paper history:
Received 19 July 2024
Received in revised form 19 September 2024
Accepted 26 September 2024

Keywords:
Hybrid Predictive Model
Bond Strength Prediction
Metaheuristic Algorithms
Neural Network
Uncertainty Quantification
Model Interpretation

A B S T R A C T

Accurate estimation of bond strength between concrete and deformed reinforcing bars is essential for the stability of reinforced concrete structures, especially in critical regions subjected to heavy loads and environmental stresses. Despite intensive experimental studies revealing the complexity of factors influencing bond strength, existing predictive models, often reliant on artificial neural networks, have limitations in accuracy due to constrained datasets and inadequate representation of real-world stress fields. In response, this study pioneers a novel hybrid metaheuristic-optimized neural network model to swiftly and precisely predict bond strength under tensile load. Utilizing a comprehensive dataset comprising 558 valid experimental outcomes, seven metaheuristic algorithms are employed to optimize the ANN architecture. These metaheuristic algorithms include the Weighted Mean of Vectors, Grey Wolf Optimizer, Energy Valley Optimizer, Circle Search Algorithm, Artificial Ecosystem-Augmented Optimization, War Strategy Optimization, and Brown-Bear Optimization Algorithm. Results demonstrate that the developed hybrid models, particularly the artificial neural networks optimized by the Weighted Mean of Vectors algorithm, exhibit superior predictive performance. This model also demonstrated the lowest miscalibration value, followed by Circle Search Algorithm and Energy Valley Optimizer, indicating a high level of reliability. Moreover, comparison with common analytical and empirical formulations revealed significant performance improvements of the proposed model, achieving a 25% reduction in MSE during the testing phase. Additionally, the Shapley Additive explanations and Sobol sensitivity analysis framework was used to interpret the proposed predictive model, highlighting key predictors such as cross-sectional area, development length or splice, reinforcing bar diameter, and concrete compressive strength.

***doi**: 10.5829/ije.2025.38.05b.19*

Graphical Abstract

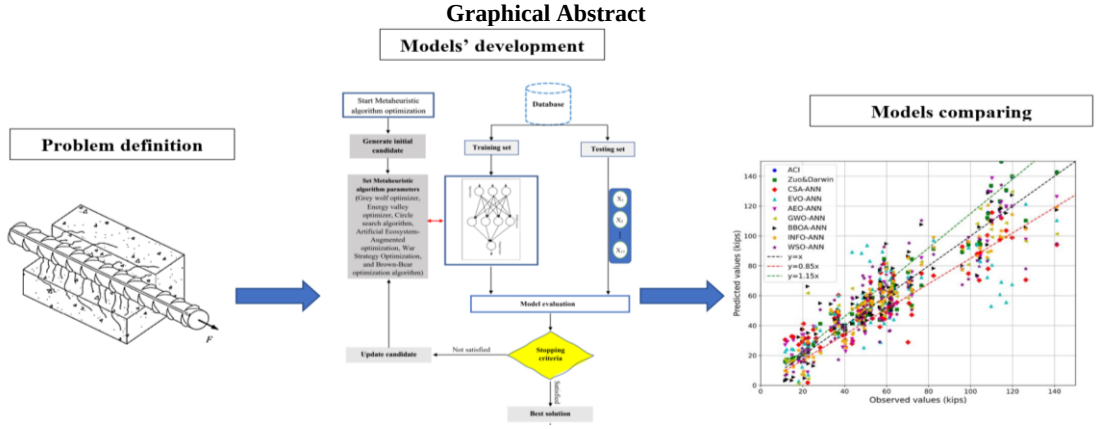

*Corresponding Author Email: nsafaeian@buqaen.ac.ir (N. Safaeian)

Please cite this article as: N. Safaeian Hamzehkolaei, S. Ghavaminejad, M. S. Barkhordari. Predictive Model of Bond Strength in Reinforced Concrete Structures: A Hybrid Metaheuristic-optimized Neural Network Approach. International Journal of Engineering, Transactions B: Applications. 2025;38(05):1190-1212

1. INTRODUCTION

The interaction between concrete and reinforcing bars is a crucial component that supports the robustness and usability of concrete structures (1). This bond-complex structure has a major impact on structural integrity, which makes it a crucial component in guaranteeing the affordability and safety of concrete structures (2). Critical areas of a reinforced concrete structure are the splice and anchorage regions, where the link between the concrete and reinforcing bars must survive heavy loads and possible environmental stresses (3). The strength of this bond determines the structural stability of buildings, bridges, and other concrete structures (4). A mistake or omission in estimating bond strength could result in structural weaknesses, jeopardizing the building's overall safety (5). Because of this, engineers and researchers are always looking for new approaches and models to improve the prediction of bond strength since they understand how important it is to the stability and longevity of reinforced concrete structures. The intricacy of factors influencing bond strength has been revealed via years of intensive experimental study (6).

Because of this relationship's complexity, it is extremely difficult to forecast bond strength. Though a number of research projects have shown impressive results, the hunt for a thorough theory-based model to forecast bond strength is still ongoing (7-9). In the lack of such a model, empirical descriptive equations that approximate binding strength have been developed (8-10). These formulas, which are the result of regression analysis of the experimental data, attempt to capture the various elements that affect the bond strength. Even though scientists have come a long way in comprehending the complexities of bond behavior, the area is still without a widely recognized and accurate predictive model (11). Machine Learning (ML) is another approach that encompasses the utilization of algorithms to construct models using available data (12, 13). When meticulously developed, these models serve as a means to unveil concealed relationships among variables influenced by the underlying principles of physics (14, 15). Researchers have adeptly applied ML algorithms across various facets of structural engineering (16), demonstrating their effectiveness in predicting pivotal parameters like the bond strength between reinforcing bars and concrete (17, 18).

This study introduces a novel hybrid metaheuristic-optimized neural network model that distinguishes itself from existing research. Unlike previous studies that primarily utilized traditional Artificial Neural Networks (ANNs) with limited optimization techniques, this research employs a hybrid model integrating seven distinct metaheuristic algorithms—INFO, GWO, EVO, CSA, AEO, WSO, and BBOA—to optimize the ANN architecture. The hybrid approach results in a significant improvement in predictive accuracy, reducing the Mean Squared Error (MSE) by 25% during the testing phase compared to existing models. Additionally, the study leverages an extensive dataset of 558 valid experimental outcomes from the Joint ACI-ASCE Committee 408 database, which is more comprehensive than those typically used in prior research. This comprehensive dataset allows for more accurate and reliable prediction of bond strength by considering a broader range of variables. A key innovation is the incorporation of the Shapley Additive explanations (SHAP) and sensitivity analysisframework for model interpretation. This integration provides transparency to the model's predictions by highlighting critical predictors such as cross-sectional area, development length, bar diameter, and concrete compressive strength, an aspect often overlooked in existing studies. Furthermore, the results demonstrate that the INFO-ANN model exhibits superior predictive performance compared to traditional ANN and analytical models. This improvement is attributed to the novel hybrid approach, which effectively combines the strengths of multiple metaheuristic algorithms. These contributions underscore the uniqueness of this research and its advancement of predictive modeling in the field.

The remainder of this paper is structured as follows: Section 2 is the literature review; Section 3 presents the experimental database; section 4 details the methodology, including the design and implementation of the hybrid metaheuristic-optimized neural network model; section 5 discusses the results, providing a thorough analysis of the model's performance, comparison with existing models, interpretation using the SHAP framework, and the sensitivity analysis results; and section 6 concludes the paper by summarizing the key findings, discussing the implications of the results, and suggesting potential areas for future research.

2. LITERATURE REVIEW

Dahou et al. (19) developed two distinct Artificial Neural Network (ANN) models to predict the pullout strength of small-diameter bars (0.39 and 0.42 inches). The first model, 6-10-1, utilized six input variables and a hidden layer with 10 neurons, while the second model, 2-4-1, employed only two input variables and four neurons in the hidden layer. Both models were trained and tested using a dataset of 112 pullout test results, with the 6-10-1 model demonstrating higher predictive accuracy compared to the 2-4-1 model.

Nguyen et al. (20) examined how corrosion influences the strength of the bond between rebar and concrete in reinforced concrete structures. To comprehend the process underlying the corrosion-induced decrease of bond strength, the researchers performed tension pull-out experiments. Based on the

experimental outcomes, they generated a preliminary dataset. They added more examples from the body of existing literature, so expanding this dataset even further. They created a powerful machine learning model called the Bayesian Regularized Feed-Forward Neural Network (BR-FFNN) to evaluate the bond behavior of corroded reinforcement using this extensive dataset.

Golafshani et al. (21) advanced the integration of ML methods with structural engineering by developing models using Fuzzy Logic (FL) and ANN to predict the bond strength of bars in concrete. These models utilized six inputs and one output, considering factors such as splice length, relative rib area, and concrete compressive strength. The ANN model, featuring a single hidden layer with 10 neurons, demonstrated slightly better predictive accuracy compared to the fuzzy logic model when tested against a dataset of 179 splice beam tests. Both models, however, showcased strong predictive capabilities and generalization, highlighting the potential of ML techniques in enhancing our understanding and predictive abilities in structural engineering.

A complex hybrid model combining a genetic algorithm and ANN was presented by Rinchon et al. (22) to evaluate the pullout bond strength of bars. Using one hidden layer with four neurons and the final bond strength as the output parameter, the model incorporates six crucial input variables (concrete compressive strength, concrete cover, bar diameter, embedment length, rib height, and rib spacing). Huang et al. (23) concentrated on creating a trustworthy model to forecast the strength of the link between concrete and corroded reinforcement. In order to predict interface bond strength using a variety of input variables, including corrosion level, reinforcement diameter, concrete cover ratio, bond length ratio, reinforcement yield strength, and concrete compressive strength, they compiled data from earlier experiments and developed a Back Propagation ANN (BP-ANN) model. The 166 groups of pull-out test data were used to train and evaluate the model. When compared to conventional empirical or semi-empirical models, the results demonstrated that the BP-ANN model's predictions were more accurate in matching the actual values. Sensitivity study revealed that bond strength is largely influenced by corrosion level, whereas reinforcement yield strength is barely affected.

Support Vector Regression and ANN models were developed by Ahmad et al. (24) for predicting the bond strength of reinforced concrete. Essential input parameters for the models' design were minimum and maximum concrete coverings, bar diameter, splice length, and concrete compressive strength. Both the ANN models, which is composed of one hidden layer with eleven neurons, and the SVR model were subjected to rigorous hyperparameter optimization by iterative grid searches. A tenfold cross-validation was applied to a dataset of 267 test outcomes to evaluate the model's effectiveness. Both models excelled in strength prediction, but the ANN model was slightly more accurate than the SVR model.

In a collaborative effort, Degtyarev (25) introduced created a neural network to forecast the bond strength between straight deformed reinforcing bars and concrete under tension loading. The model was constructed using a vast dataset sourced from the Joint ACI-ASCE Committee 408 database. This model utilized 408 databases from the Joint ACI-ASCE Committee to capture the intricate relationships among variables influencing bond strength. This initiative substantially enhanced the predictive abilities in bond strength assessment by leveraging a rich repository of experimental data for model development.

The review of existing literature underscores the limited application of ML techniques in predicting bond strength, with a predominant reliance on ANNs. Previous models often stem from relatively constrained datasets, characterized by restricted feature ranges and reliance on pullout test specimens. Critically, the latter is cautioned against by Joint ACI-ASCE Committee 408 (26), as these specimens inadequately reflect the authentic stress fields encountered in typical structures. To address these gaps, this study aims to develop an efficient hybrid metaheuristic-optimized neural network model for swift and precise predictions of bond strength, utilizing seven distinct metaheuristic algorithms to optimize the ANN.

3. EXPERIMENTAL DATABASE

The dataset employed in this investigation was derived from the Joint ACI-ASCE Committee 408 database (7, 26), which encompasses a comprehensive collection of 635 experimental outcomes pertaining to the development length and splice strength of uncoated deformed reinforcement bars. This database meticulously catalogues a diverse array of design parameters that are critical to the assessment of bond strength between concrete and steel reinforcement. It encompasses the quantification of ultimate tensile stresses in reinforced bars, these being ascertained through the analysis of beam tests via two predominant methodologies: the moment-curvature technique and the working stress approach. It is pertinent to note that the analysis specifically discounted any test results devoid of values needed for the moment-curvature technique and the working stress approach, thereby refining the dataset to 558 valid experimental outcomes. This curation process ensures the reliability and specificity of the dataset in analyzing the bond strength with a focus on variables that significantly impact the structural integrity of reinforced concrete elements.

The variables introduced into the analysis encompass a range of geometric and material properties, critical for evaluating the bond mechanics between concrete and reinforcing steel. These parameters include the length of

development or splice (l_s); the diameter of the reinforcing bar (d_b); the relative rib area (R_r), serving as a quantifier for the mechanical interlock effectiveness; the minimum ($C_{\min}$) and maximum ($C_{\max}$) concrete covers, delineating the protective concrete layer thickness around the reinforcement; the number of reinforcing bars subjected to development or splicing (N_b); the count of transverse reinforcements—either stirrups or ties—positioned within the specified length of development or splice (N_s); the cross-sectional area of the bar under consideration (A_b); the cross-sectional area of each transverse reinforcement element (A_t); and the compressive strength of concrete (f_c). The focal outcome of this analytical framework is the bond force (F_b), which is extrapolated as a function of the aforementioned input variables, thereby providing a comprehensive measure of the bond integrity within reinforced concrete assemblies.

Figure 1 shows the correlation between different input parameters. The diagonal elements show histograms for each individual parameter. The scatter plots and correlation coefficients show the relationships between pairs of parameters. The correlation coefficient values range from -1 to 1. The correlation coefficient of 0.36 suggests a moderate to strong positive correlation between the length of development or the splice and diameter of the reinforcing bar. This implies that as the length of development or splice increases, the diameter of the reinforcing bar also tends to increase. This relationship can be attributed to the need for longer splices to accommodate larger bars, ensuring adequate anchorage and mechanical interlock. There is a slight positive correlation between the quantity of reinforcing bars and the cross-sectional area of the bar. This indicates that structures with more reinforcing bars tend to have bars with larger cross-sectional areas. The design might aim to distribute loads more effectively and improve the structural capacity. There is a moderate positive correlation (0.52) between the minimum concrete cover and the cross-sectional area of the bar. This suggests that as the minimum concrete cover increases, the cross-sectional area of the reinforcing bar also tends to increase. This relationship can be explained by several possible reasons: (1) Larger reinforcing bars (with greater cross-sectional areas) are often used in critical structural elements that require increased protection. Consequently, these elements might be designed with greater minimum concrete cover to ensure durability and protect against environmental factors such as corrosion and (2) Increased concrete cover helps in controlling crack widths, especially in structures exposed to aggressive environments. Larger bars might be associated with sections where crack control is crucial, necessitating an increase in the concrete cover.

4. METAHEURISTIC-OPTIMIZED ARTIFICIAL NEURAL NETWORK (ANN)

The architecture and parametrization of ANN models, particularly the number of hidden layers and connection weights between neurons, significantly impact their performance (27, 28). Suboptimal architectures can lead

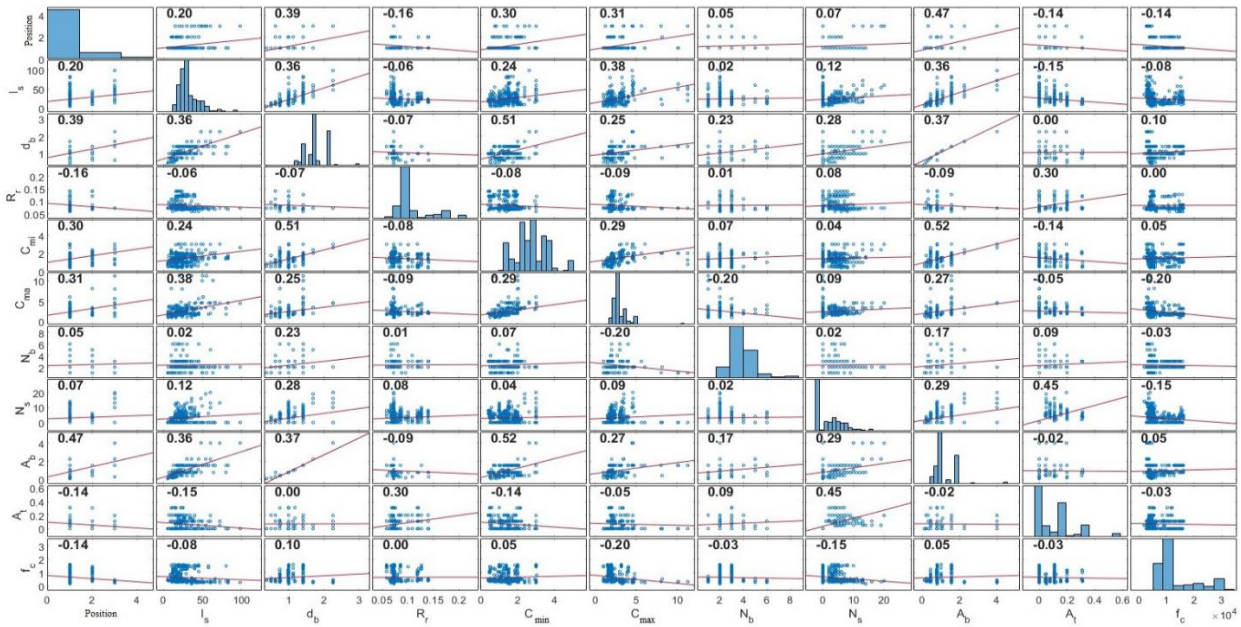

Figure 1. Correlation between different input parameters

to issues like underfitting, overfitting, or poor generalization, adversely affecting predictive accuracy and computational efficiency (27). Optimizing ANN designs is crucial for achieving higher performance and faster convergence (28, 29). In addition, metaheuristic algorithms are powerful global optimization techniques inspired by natural or human phenomena, proficient at tackling intricate optimization issues with extensive search spaces that are challenging for traditional methods (29). For complex optimization problems, common gradient descent-based backpropagation algorithm and other gradient-based algorithms may not always yield accurate optimal solutions (30, 31). Hence, researchers frequently hybridized machine learning models with metaheuristic algorithms to enhance the robustness and predictive capabilities of the predictive models (31, 32).

Metaheuristic algorithms facilitate an effective search through diverse hidden layer configurations by exploring the solution space and evaluating each candidate architecture against predefined fitness criteria. Determining the optimal number and size of hidden layers is vital for striking the right balance between model complexity and generalization performance (28, 32). Moreover, the optimal weight configuration should also be identified to minimize the discrepancy between the network's predicted outputs and the actual targets in the training data. In this study, metaheuristic algorithms are employed to tune automatically the hyperparameters of the ANN-based predictive model, e.g., the number of neurons in the single hidden layer, connection weights, and biases of a shallow neural network architecture. Figure 2 shows the flowchart of the proposed metaheuristic-optimized ANN models for bond strength prediction in reinforced concrete structures. For this purpose, seven distinct optimization algorithms, including the Grey wolf optimizer (GWO), Energy valley optimizer (EVO), Circle search algorithm (CSA), Artificial Ecosystem-Augmented optimization (AEO), War Strategy Optimization (WSO), and Brown-Bear optimization algorithm (BBOA), are utilized. According to Figure 2, during the ANN-based model optimization procedure, an effective search is performed for the ideal weight values and number of neurons by treating them as unknown variables in the optimization process. Details of the utilized optimization algorithms are presented in the next subsections.

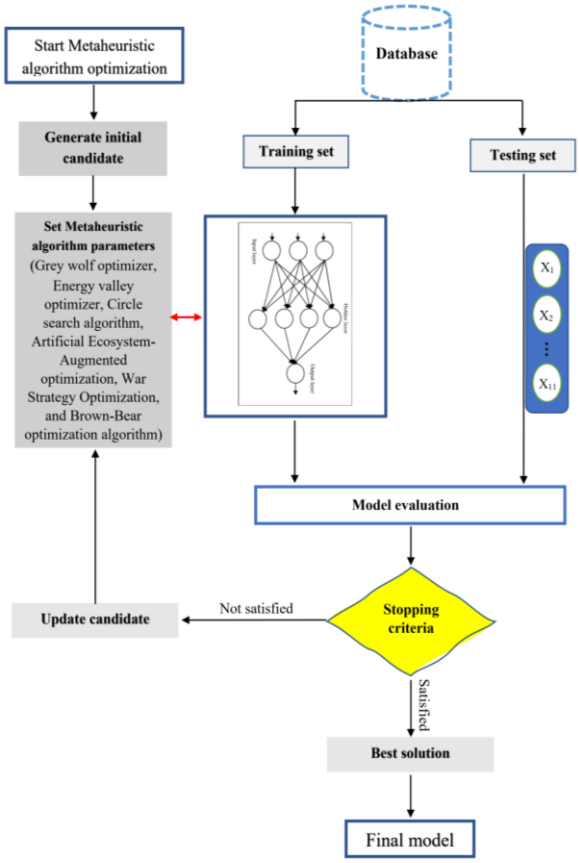

Figure 2. Flowchart of the optimized ANN model

4. 1. Grey Wolf Optimizer (GWO) The GWO, one of these metaheuristic algorithms, is distinguished by its efficacy, simplicity, and natural inspiration. GWO, which was created by Mirjalili et al. (33), improves candidate solutions repeatedly by imitating the social structure and hunting techniques of grey wolves. The idea of the Grey Wolf Optimizer is to mimic the social dynamics and hunting behavior seen in a pack of grey wolves. Within their pack, greyhounds naturally display a hierarchical structure, with alpha, beta, delta, and omega wolves signifying varying degrees of authority. To effectively pursue and catch prey, pack members must cooperate and coordinate their hunting approach. In order to convert this behavior into an optimization algorithm, GWO models possible solutions as members of a wolf pack. A position vector that represents a point in the search space distinguishes each solution, or wolf. Based on the motions of alpha, beta, delta, and omega wolves—which correspond to the best solutions found so far—the program iteratively adjusts these placements. The following is a mathematical expression for the Grey Wolf Optimizer (33):

Step 1: Starting Point: Create a population of wolves from the beginning, with each wolf representing a possible fix for the optimization issue. Assign the wolves in the search area with random starting positions.

Step 2: Assessment of Fitness: Based on where each wolf is located in the search space, determine how fit they are. The objective function of the optimization problem is matched by the fitness function.

Step 3: Social Structure: Determine the fitness values of the alpha, beta, delta, and omega wolves. These wolves stand in for the greatest fixes found during the most recent iteration.

Step 4: Exploration as well as Abuse: Three basic equations that model exploration and exploitation are used to update each wolf's position. Equation 1 updates the alpha wolf's location. Equation 2 recalculates the beta, delta, and omega wolves' locations. Equation 3 revises the remaining wolves' locations.

$$X^{\alpha}(t+1) = X^{\alpha}(t) - \alpha \cdot D \tag{1}$$

$$X^{i}(t+1) = X^{\alpha}(t) - \beta \cdot D \tag{2}$$

$$X^{i}(t+1) = X^{\alpha}(t) - \gamma \cdot D \tag{3}$$

where $X^{\alpha}(t+1)$ represents the updated position of the alpha wolf at iteration $t+1$, $X^{i}(t+1)$ represents the updated position of the i-th wolf at iteration $t+1$, $X^{\alpha}(t)$ represents the current position of the alpha wolf at iteration t, D is a random vector, and α, β and γ are scaling factors controlling the exploration and exploitation phases.

Step 5: Boundary Handling: Make sure the wolves' updated locations stay inside the boundaries of the search area. If required, use the proper boundary handling strategies.

Steps 2 through 5 should be repeated until a termination criterion—such as a maximum number of iterations or convergence to a workable solution—is satisfied.

4. 2. Energy Valley Optimizer (EVO) In this section, the paradigm of the EVO (34) is explained as a complexly designed optimization algorithm explained by applying the principles of theoretical physics established. In the realm of physical reactions, particles collide to generate new particles, and while the majority of particles in the universe are assumed to be unstable, a subset of stable particles remains unchanged over time. Unstable particles undergo decay, emitting energy, with varying decay rates across particle types. The concept of an energy valley relates to particle stability based on binding energy and interactions. Expert observations have identified patterns in particle decay. Key challenges include determining stability based on neutron (N) and proton (Z) counts and the N/Z ratio. A N/Z ≈ 1 indicates stability for lightweight particles, while heavier ones achieve stability with a higher N/Z value. Particle stability levels are influenced by neutron enrichment, and particles above the stability bound undergo decay, requiring additional neutrons for stability. At the beginning of the initial phase, the initialization process unfolds, where the solution candidates (X_i) are conceptualized as quasi-particles with different stability properties within the defined search space. This search space is postulated to be a limited sector of a broader cosmic domain:

$$X = \begin{bmatrix} X_1 \\ X_2 \\ \vdots \\ X_n \end{bmatrix} = \begin{bmatrix} x_1^1 & \cdots & x_1^d \\ \vdots & \vdots & \vdots \\ x_n^1 & \cdots & x_n^d \end{bmatrix}, \quad \begin{cases} i = 1,2.,...,n \\ j = 1,2,...,d \end{cases} \tag{4}$$

$$x_i^j = x_{i,\min}^j + rand(x_{i,\max}^j - x_{i,\min}^j), \quad \begin{cases} i = 1,2.,...,n \\ j = 1,2,...,d \end{cases} \tag{5}$$

where n refers to the total number of particles and refers to the entire set of candidate solution that live in the vast universe and serve as defined search space, d expresses the dimension of the problem considered and the scope of the variables in play. The symbol x_i^j represents the decision variable j[th] used to determine the initial spatial configuration of the candidate i[th] particle. The pairs of $x_{i,\min}^j$ and $x_{i,\max}^j$ represent the lower and upper limits of the jth variable within the ith candidate, establishing the range of values allowed for the decision variable, respectively. The rand symbol represents the uniform distribution of random numbers from intervals [0, 1] and acts as a stochastic element in the initialization process, thus contributing to the diversification of the initial position of particles.

In the next phase of the algorithm, a particle enrichment boundary (EB) is determined and serves as an important metric for determining the disparity between neutron-rich particles and neutron-poor particles in the system. This includes the evaluation of the objective functions of each particle, thereby determining the neutron enrichment level (NEL) shown by each particle. The formal expression that encapsulates these aspects is expressed as follows:

$$EB = \frac{\sum_{i=1}^{n} NEL_i}{n}, \; i = 1,2,...,n \tag{6}$$

In the specified formulation, NEL_i signifies the Neutron Enrichment Level exhibited by the ith particle, and EB denotes the Enrichment Bound characterizing the neutron enrichment levels across the entire population of particles within the universe. In the subsequent procedural step, the quantification of particle stability levels ensues, predicated on the evaluations derived from the objective function. The method for determining these stability levels is elucidated as follows:

$$SL_i = \frac{NEL_i - BS}{WS - BS}, \quad i = 1,2,...,n \tag{7}$$

In this context, SL_i designates the stability level attributed to the ith particle, while BS and WS represent particles characterized by the most favorable and least favorable stability levels within the universal context.

These particles correspond to instances featuring the minimum and maximum values encountered thus far in the evaluation of the objective function. Within the primary search loop of the Evolutionary Optimization (EVO), if a particle's neutron enrichment level surpasses the enrichment bound ($NEL_i > EB$), indicating the potential for decay processes is considered. Towards the conclusion of the principal loop in the Evolutionary Optimization (EVO), only two fresh position vectors are generated for each particle if its enrichment level exceeds the predefined enrichment bound. Conversely, if the particle exhibits a lower enrichment level, only a single position vector, is generated anew. Subsequently, at each stage, the newly generated vectors are integrated into the existing population, and the superior particles actively partake in the ensuing iteration of the algorithm's search loop. A flag is established to identify boundary violations for decision variables that extend beyond the predetermined upper and lower bounds. Additionally, termination criteria can include either a maximum number of objective function evaluations or a maximum number of iterations.

4. 3. Circle Search Algorithm (CSA) CSA (35) is a metaheuristic algorithm inspired by natural events, namely the circular search patterns that some species display when they are scavenging or exploring. CSA attempts to effectively search the solution space and identify potential places where optimum solutions might exist by imitating this behavior. The Circle Search Algorithm works on the basis of doing circular searches inside the solution space iteratively. The algorithm may methodically investigate different regions while gradually convergent towards promising solutions thanks to this circular search technique. Each candidate solution is represented as a point in the search space, and the algorithm keeps track of a population of these points. CSA performs circular searches around each potential solution's present position at each iteration. The algorithm is able to achieve a balance between exploring new regions and exploitation of promising areas by dynamically adjusting the circular search's radius based on the exploration-exploitation balance. The Circle Search Algorithm can be represented mathematically in the following way:

1. Initialization: Create randomly generated positions at the beginning of a population of candidate solutions S in the search space. Establish parameters like the maximum search radius, the number of iterations, and the convergence criteria.
2. Fitness Evaluation: Based on the optimization problem's objective function, assess each potential solution's fitness within the population.
3. Circular Search: In the population S, for every potential solution s_i: 1) Based on the exploration-exploitation balance and the position of s_i in relation to other solutions, determine the search radius, r_i, 2) To investigate nearby areas, do a radial search with radius r_i around s_i's present location, and 3) Using the best answer found during the circular search, update the location of s_i.

A formula based on the exploration-exploitation balance may be used to dynamically compute the search radius (ri) for each possible solution (si). The following is one way to modify the search radius:

$$r_i = \frac{R_{\max}}{1 + e^{-(kt-c)}} \tag{8}$$

where $R_{\max}$ is the maximum search radius, k is a scaling factor controlling the rate of adjustment, c is a constant term influencing the shape of the adjustment curve, and t is the current iteration.

4. Exploration and Exploitation: To strike a balance between the exploitation of potential areas and the investigation of new ones, dynamically adjust the search radius. Heuristics based on the algorithm's performance and convergence state or adaptive techniques can be used to accomplish this.
5. Termination Criterion: Steps 2-4 should be repeated until a termination requirement is satisfied, such as attaining convergence to a workable solution or reaching a maximum number of iterations.

4. 4. Weighted Mean of Vectors (INFO) Collections of vectors representing various observations, measurements, or features are frequently encountered in real-world scenarios. These vectors may have different degrees of significance or applicability to the overall analysis. The Weighted Mean of Vectors (INFO) (36) offers a way to combine these vectors into a single representative vector while accounting for their individual weights. The Weighted Mean of Vectors (INFO) functions according to the idea that weights are allocated to each vector in the collection according to its importance or input. Depending on the particulars of the situation, these weights may be established empirically, via optimization techniques, or based on past information. The Weighted Mean of Vectors (INFO) can be mathematically expressed as follows:

$$INFO = \frac{\sum_{i-1}^{n} w_i \cdot v_i}{\sum_{i-1}^{n} w_i} \tag{9}$$

where v_i is a vector representing various observations, measurements, or features and w_i is the vector corresponding weight, and INFO represents the weighted mean vector. To guarantee that the final vector has a unit weight, the denominator normalizes the result by adding the weights of the vectors that the numerator computed.

In some cases, weights can be calculated based on the inverse of the variance or uncertainty associated with each vector. Let σ_i^2 represent the variance of the vector v_i. The weights can be calculated as:

$$w_i = \frac{1}{\sigma_i^2} / \sum_{i-1}^{n} \frac{1}{\sigma_i^2} \quad (10)$$

INFO is superior to other aggregation techniques or simple averaging in a number of ways. 1) Flexibility: Enables weighting systems to be adjusted to represent the relative relevance of different vectors; 2) Robustness: Able to handle vectors with varying scales and dimensions by using the right normalizing methods; 3) Interpretability: Gives the concatenated vectors, including their weights and values, a clear visual representation; and 4) Efficiency: Computationally efficient, needing only simple arithmetic operations for a simplistic implementation.

4. 5. Artificial Ecosystem-Augmented Optimization (AEO) The intricate dynamics and self-organizing characteristics of real ecosystems serve as the inspiration for the revolutionary metaheuristic method known as AEO (37). AEO explores and exploits the solution space of optimization problems repeatedly by imitating the concepts of symbiosis, competition, and adaptability found in ecosystems. Numerous disciplines, including engineering, economics, biology, and more, deal with optimization issues. It is frequently difficult for traditional optimization methods to navigate high-dimensional, nonlinear, and multimodal solution spaces. Natural events have served as the inspiration for metaheuristic algorithms, which have become effective instruments for overcoming these difficulties. Among these algorithms, AEO optimization stands out for its novel methodology, which takes inspiration from the dynamic interactions seen in natural ecosystems.

The principles of real ecosystems, where organisms interact with one another and their surroundings to live and prosper, provide as the foundation for the conceptual framework of Artificial Ecosystem Augmented (AEO) optimization. To address optimization issues, AEO analyzes the essential dynamics of ecosystems, such as symbiosis, competition, and adaptability. Candidate solutions are modeled in the AEO framework as individuals within a population, much like animals in an ecosystem. Through a process of crossover, mutation, and selection, these individuals interact with one another and change over the course of subsequent generations.

The AEO optimization algorithm can be mathematically formulated as follows: 1) Initialization: Establish a population of candidate solutions, each of which represents a potential fix for the optimization issue. Assign each member of the population a random starting position. 2) Assessment of Fitness: Determine each population member's level of fitness by looking at where they fall in the solution space. The objective function of the optimization problem is matched by the fitness function. 3) Symbiosis and Competition: Select individuals from the population based on their fitness scores to serve as parents for reproduction. The probability of selection is proportional to the individual's fitness. Foster symbiotic relationships amongst people to enhance communication and collaboration. Mechanisms like crossover and information exchange can help achieve this. 4) Encourage individual rivalry to promote discovery and avert early convergence. Selection processes that favor persons with greater fitness levels can be used to mimic competition. 5) Adaptation and Evolution: Produce children with a variety of traits by utilizing evolutionary operators like mutation and reproduction. Provide systems for maintaining population control and variety so that people may adjust to changing environmental conditions. 6) Termination Criterion: Repeat steps 2-4 until a termination criterion is met. The equations governing the reproduction and environmental interaction processes in AEO can be represented as follows:

-Selection Probability:

$$P_i = \frac{f_i}{\sum_{j=1}^{N} f_j} \quad (11)$$

where P_i is the probability of selecting an individual i as a parent, f_j is the fitness of the individual i, and N is the population size.

-Mutation Operation:

$$x_{ij}^{'} = x_{ij} + \Delta x_{ij} \quad (12)$$

Where $x_{ij}^{'}$ is the mutated value of the jth gene of the individual i, x_{ij} is the original value of the jth gene of individual i, and Δx_{ij} is a random perturbation added to the gene value.

-Survival Selection:

$$P_{survival} = \min(1, \frac{f_{offspring}}{f_{parent}}) \quad (13)$$

Where $P_{survival}$ is the probability of an offspring surviving to the next generation, $f_{offspring}$ is the fitness of the offspring, and f_{parent} is the fitness of the parent.

4. 6. War Strategy Optimization (WSO) The history of humanity has revolved around warfare, and

battle tactics have changed dramatically throughout time. From open-field battles in antiquity to sophisticated tactics and cutting-edge technology in contemporary warfare, the objective has always been to maximize strategies for victory while reducing losses and resource consumption. The way military operations are planned and carried out has changed dramatically in recent years due to the incorporation of computer methodologies and mathematical models. One such development is the multilayered WSO algorithm (38), which improves military decision-making by utilizing mathematical principles and algorithms.

Fundamentally, WSO uses mathematical models to examine a range of variables, including troop movements, topography features, enemy behavior, and resource distribution, in an effort to solve the complexity of combat. Military strategists can learn the best tactics and techniques by quantifying these variables and putting them into mathematical formula. Using game theory, a field of mathematics that examines the strategic interactions between rational decision-makers, is a key component of WSO. Game theory allows analysts to describe conflicts in the context of warfare as strategic games in which the decisions made by each player affect the outcomes for all sides. Originally designed to help in zero-sum game decision-making, equations like the minimax algorithm are now used to determine the optimal course of action in military situations (38).

$$Minimax\ Algorithm:\ max_a min_b Utility(a,b) \tag{14}$$

where a represents the actions of one player, b represents the actions of the opponent, and $Utility(a,b)$ quantifies the outcome based on the actions of both players. By iteratively optimizing strategies through this algorithm, military commanders can anticipate and counter potential enemy moves, thereby gaining a strategic advantage on the battlefield. In addition, WSO uses mathematical optimization methods to handle logistical issues and resource distribution. For example, linear programming is used to effectively distribute scarce resources like labor, fuel, and ammunition. The intended result is represented by the objective function in this case, while resource allocations are kept within predetermined bounds by constraints. Military planners can ascertain the best way to allocate resources in order to facilitate combat operations by using linear programming models. Furthermore, WSO uses network theory to examine the interconnectedness and susceptibility of supply chains, communication networks, and military infrastructure. Resilience algorithms, centrality metrics, and network flow equations are used to determine possible weaknesses that adversaries can exploit and to evaluate how resilient critical infrastructure is:

$$\begin{aligned}
&Network\ Flow: \sum_{i,j} Flow_{i,j} - \sum_{i,j} Flow_{j,i} = \\
&Supply_i - Demand_i \\
&Centrality\ Measures: Centrality(v) = \\
&\sum_{s \neq v \neq t} \frac{Shortest\ Path(s,t;v)}{Shortest\ Path(s,t)} \\
&Resilience\ Algorithm: Resilience(G) = \\
&\frac{Number\ of\ Disconnected\ Nodes}{Total\ Nodes}
\end{aligned} \tag{15}$$

Military planners can find critical nodes in a network that, if compromised, could seriously affect the enemy's capacity to plan and carry out military actions by using network theory. Furthermore, WSO combines modeling and simulation methods to create plausible scenarios and evaluate the possible results of various tactics. To replicate troop movements, combat encounters, and battlefield dynamics, discrete event simulations, agent-based modeling, and Monte Carlo simulations are used. Before making choices in the field, military commanders can use these simulations to investigate "what-if" situations, assess the efficacy of alternative plans, and reduce risks:

$$\begin{aligned}
&Agent-based\ Modeling: Agent_i = \\
&f(Environment, Neighboring\ Agents, Internal\ State) \\
&Monte\ Carlo: Outcome = \\
&(Num.of\ Successful\ Simulations / Total\ Simulations) \\
&Discrete\ Event\ Simulation: \\
&Events(t) = Events(t-1) + New\ Events
\end{aligned} \tag{16}$$

Military strategists may improve their comprehension of combat dynamics, spot possible risks and weaknesses, and adjust their operations accordingly by integrating simulation and modeling approaches.

4. 7. Brown-Bear Optimization Algorithm (BBOA)

The BBOA is a paradigm that is intriguing and draws inspiration from the complex workings of nature (39). Based on the actions of the brown bear, a powerful animal known for its ability to adapt, BBOA is an amalgam of biological knowledge and computer techniques designed to address challenging optimization issues in a variety of fields. Fundamentally, BBOA takes its cues from brown bears' foraging habits as they seek their surroundings for food sources. Similar to how these bears traverse a variety of landscapes in order to obtain food, BBOA designs a search strategy that strikes a balance between exploitation and exploration in order to identify the best answers. The algorithm uses features like random exploration and local exploitation to effectively converge toward plausible solutions, emulating the adaptive methods of brown bears. The BBOA can be formulated as follows (39):

Given: $F(x)$ is the objective function to be minimized or maximized, x_i is the position of the ith bear in the search space, X_{best} is the best solution found so far, v_i is the velocity of the ith bear, P_{attack} is the probability of attack, and P_{scout} is the probability of scouting for a new solution; the algorithm is:

1. Initialization: Initialize bear positions randomly within the search space.
2. Evaluation: Evaluate the objective function for each bear.
3. Update X_{best}: Update the best solution found so far.
4. For each bear i:

- Calculate velocity (v_i).

$$v_i(t+1) = v_i(t) + c_1 \cdot rand() \cdot (X_{best} - x_i(t)) \quad (17)$$

where c_1 is the learning coefficient and rand() generates a random number between 0 and 1.

- Update bear position (x_i).

$$x_i(t+1) = x_i(t) + x_i(t+1) \quad (18)$$

- Apply attack behaviour with probability (P_{attack}).

$$x_i(t+1) = x_i(t+1) + rand() \cdot (x_i(t) - X_{best}) \quad (19)$$

- Apply scouting behaviour with probability (P_{scout}).

$$x_i(t+1) = x_{rand} \quad (20)$$

where x_{rand} is a randomly generated position within the search space.

5-Repeat steps 2-4 until termination criteria are met.

4. 8. Performance Assessment To rigorously evaluate the machine learning (ML) model's performance, a comprehensive assessment was conducted employing widely accepted and statistically robust evaluation metrics. Specifically, the Mean Absolute Error (MAE, Equation 21), Mean Squared Error (MSE, Equation 22), and Coefficient of Determination (R^2, Equation 23) were utilized. These metrics provide a quantitative and objective measure of the model's predictive capabilities by systematically quantifying the deviations between the observed and predicted values across the entire dataset. The MAE and MSE metrics offer insights into the average magnitude of errors, with the MSE further emphasizing larger errors due to the squaring operation. Conversely, R^2 elucidates the proportion of variance in the target variable that can be accounted for by the model's predictions, thereby assessing the goodness-of-fit. Collectively, these evaluation criteria furnish a comprehensive and statistically rigorous assessment of the ML model's performance, enabling informed comparisons and facilitating the selection of the most accurate and reliable model for the given predictive task.

$$MAE = \frac{1}{k}\sum_{i=1}^{k}|O_i - P_i| \quad (21)$$

$$RSME = \frac{1}{k}\sum_{i=1}^{k}(O_i - P_i)^2 \quad (22)$$

$$R^2 = 1 - \frac{\frac{1}{k}\sum_{i=1}^{k}(O_i - P_i)^2}{\frac{1}{k}\sum_{i=1}^{k}(O_i - \bar{P}_i)^2} \quad (23)$$

where O_i, P_i, $\bar{P}_i$, and k are the measured values, calculated values, average of the values, and the number of the samples, respectively.

5. RESULTS AND DISCUSSION

In the initial phase of neural network architecture design, a critical consideration involves the determination of the optimal number of neurons within the hidden layer. This pivotal task entails the selection of the hidden layer neuron count as a variable parameter. Leveraging optimization algorithms, the weights of the neural network are computed across a spectrum of neuron quantities, ranging from 3 to 30. The resultant adjustments in the number of hidden layer neurons engender variations in performance metrics such as R^2, MAE, and MSE. This analysis, depicted in Figure 3, elucidates the dynamic interplay between these metrics across diverse hybrid algorithms. Each algorithm is denoted by an abbreviation followed by "-ANN" to signify its integration with ANN. Notably, this evaluation phase operates on the training dataset to iteratively refine the neural network's configuration.

These optimization methods have their own hyperparameters that significantly influence various aspects of the optimization process, including convergence, accuracy, and the ability to escape local extrema, among others. Here, the default parameters proposed in the original papers for each optimization method were employed. This approach ensures consistency with the authors' recommendations and allows for a standardized comparison across different techniques. A total of 1000 iterations and a population size of 25 were considered for all metaheuristic optimization algorithms. In addition, 80 percent of the data was randomly used for the training phase, and 20 percent of the data was allocated for the testing phase. The data was normalized and scaled to a range of 1 to -1. The search space for the weights and biases is defined within the range of -1 to 1, while the number of neurons is allowed to vary between 2 and 30.

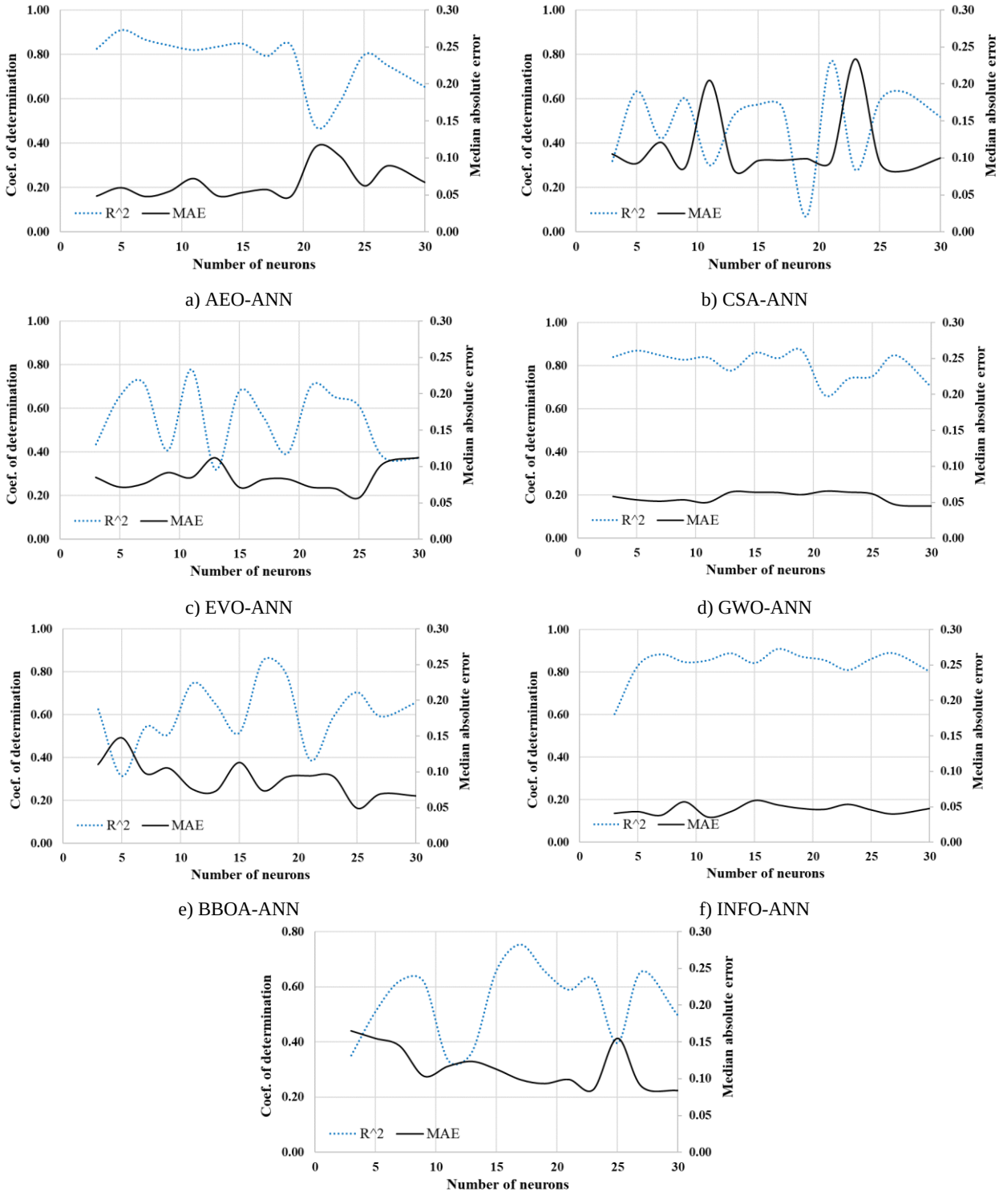

Figure 3. Training performance of the ANN with the change in the number of neurons within the hidden layer

5. 1. Comparative Analysis Table 1 presents the performance results of various hybrid algorithms employed in the context of an artificial neural network (ANN) framework with its optimal neurons. Upon scrutiny of the performance metrics, certain observations can be made:

- AEO-ANN achieved a notably low MSE of 0.00594 and low MAE of 0.06038. Its R^2 score of 0.910 indicates a high level of predictive accuracy.
- CSA-ANN and EVO-ANN exhibit similar performance in terms of MSE and MAE, with values around 0.015 for MSE and approximately 0.09 for MAE. However, their R^2 score metrics, at 0.774 and 0.773 respectively, indicate a slightly lower level of predictive accuracy compared to AEO-ANN.
- GWO-ANN and BBOA-ANN demonstrate comparable MSE and MAE metrics, with values hovering around 0.009 for MSE and 0.07 for MAE. Their R^2 score metrics, at 0.871 and 0.853 respectively, signify a relatively high predictive accuracy.
- INFO-ANN stands out with an MSE of 0.00595 and an impressively low MAE of 0.05285, matching the performance of AEO-ANN. Additionally, its R^2 score of 0.910 mirrors the high level of predictive accuracy observed in AEO-ANN.
- WSO-ANN exhibits the highest MSE among the models, at 0.01633, and also the highest MAE, at 0.09875. Its R^2 score of 0.753 suggests a comparatively lower level of predictive accuracy compared to other models.

Overall, AEO-ANN and INFO-ANN showcase superior performance across all metrics, with low MSE and MAE values accompanied by high R^2 score metrics, indicative of their strong predictive capabilities. Conversely, WSO-ANN displays comparatively poorer performance across all metrics, indicating its potential limitations in predictive accuracy.

Table 2 displays the results of performance measurement during the testing phase. Upon analysis, it is discernible that the INFO-ANN model exhibits the lowest MSE (0.00615) and MAE (0.05443) values, along with the highest R^2 score of 0.929, suggesting superior predictive accuracy and model fit compared to other algorithms. Following closely, the AEO-ANN model also demonstrates competitive performance with a relatively low MSE of 0.00697, MAE of 0.06218, and a R^2 score of 0.906. Conversely, the EVO-ANN model displays the highest MSE (0.02079) and MAE (0.10516) values, coupled with the lowest R^2 score of 0.720, indicating comparatively poorer predictive accuracy and model fit.

The WSO-ANN model similarly exhibits elevated error metrics with an MSE of 0.01633 and an MAE of 0.08945, resulting in a R^2 score of 0.780. The remaining models, namely CSA-ANN, GWO-ANN, and BBOA-ANN, present intermediary performance measures across the metrics evaluated. CSA-ANN and BBOA-ANN demonstrate relatively lower MSE and MAE compared to EVO-ANN and WSO-ANN, yet slightly inferior to AEO-ANN and INFO-ANN. GWO-ANN displays a competitive performance with a relatively low MSE of 0.00869, MAE of 0.06339, and a R^2 score of 0.883.

Overall, the results suggest that the INFO-ANN model outperforms other hybrid algorithms in terms of predictive accuracy and model fit, as evidenced by their lower error metrics and higher R^2 scores. Figure 4 illustrates the predictive capabilities of different machine learning models on both training and testing datasets.

Table 3 presents a comprehensive ranking of machine learning models based on different performance metrics. Each model's rank for MSE and MAE is listed, along with their overall performance. It is evident from this table that the INFO-ANN model consistently outperforms the others, achieving the top rank across all evaluated metrics. The AEO-ANN and GWO-ANN models also demonstrate strong performance, securing the second and third ranks, respectively, for both MSE and MAE indices. In contrast, the CSA-ANN and EVO-ANN models are at the lower end of the ranking, indicating relatively poorer performance. The BBOA-ANN model shows a slight discrepancy, performing well in some areas but not as consistently across all metrics, as reflected in its fourth and fifth ranks. The WSO-ANN model, while reliable, ranks sixth across all metrics.

TABLE 1. Models' comparison in the training phase

Model	Metrics		
	MSE	MAE	R^2
AEO-ANN	0.00594	0.06038	0.910
CSA-ANN	0.01499	0.09511	0.774
EVO-ANN	0.01503	0.08594	0.773
GWO-ANN	0.00854	0.06802	0.871
BBOA-ANN	0.00970	0.07488	0.853
INFO-ANN	0.00595	0.05285	0.910
WSO-ANN	0.01633	0.09875	0.753

TABLE 2. Models' comparison in the testing phase

Model	Metrics		
	MSE	MAE	R^2
AEO-ANN	0.00697	0.06218	0.906
CSA-ANN	0.01157	0.08134	0.844
EVO-ANN	0.02079	0.10516	0.720
GWO-ANN	0.00869	0.06339	0.883
BBOA-ANN	0.01048	0.07371	0.859
INFO-ANN	0.00615	0.05443	0.929
WSO-ANN	0.01633	0.08945	0.780

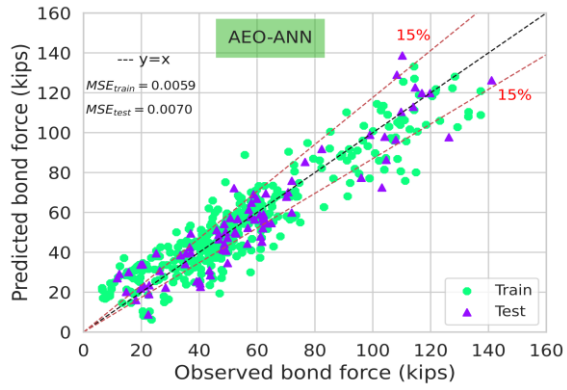

a) AEO-ANN

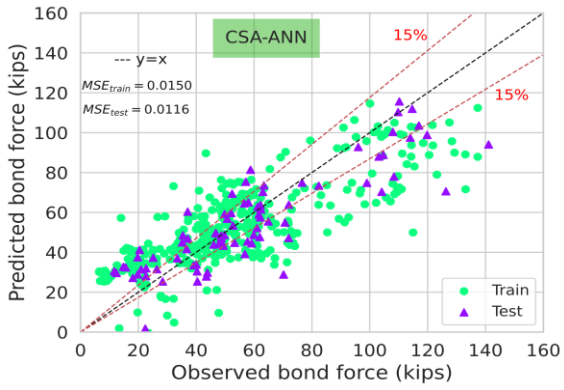

b) CSA-ANN

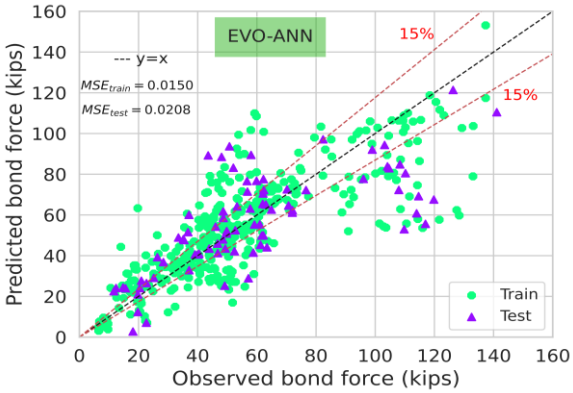

c) EVO-ANN

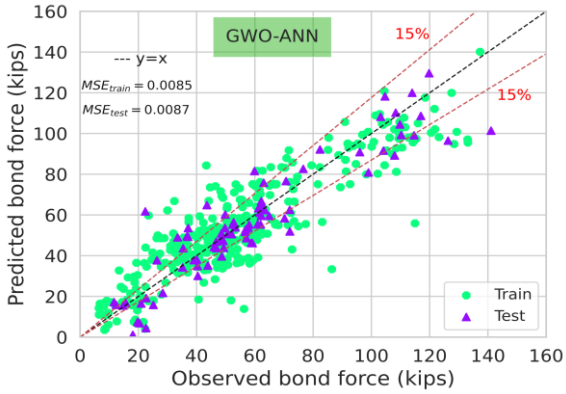

d) GWO-ANN

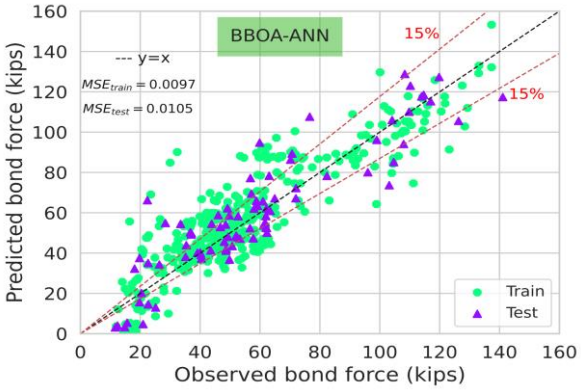

e) BBOA-ANN

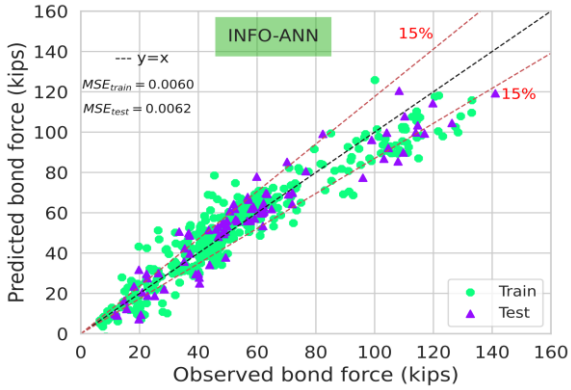

f) INFO-ANN

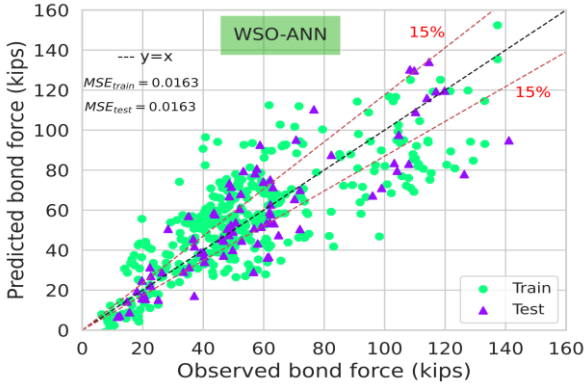

g) WSO-ANN

Figure 4. Visualization of various ML models prediction

TABLE 3. The rank of ML-based models

Model	Performance index		
	MSE	MAE	R^2
AEO-ANN	2	2	2
CSA-ANN	5	5	5
EVO-ANN	7	7	7
GWO-ANN	3	3	3
BBOA-ANN	4	4	5
INFO-ANN	1	1	1
WSO-ANN	6	6	6

These rankings highlight the superior performance of the INFO-ANN model suggest that it possesses significant predictive accuracy and generalization capabilities compared to the other models in the study.

5. 2. Uncertainty Quantification Recent breakthroughs in machine learning have significantly enhanced predictive accuracy across various disciplines (40, 41). Concurrently, the need to tackle inherent uncertainties has grown, as confident forecasts are vital for informed decision-making (31). This section employs the average calibration metric and adversarial group calibration metric to evaluate predictive uncertainty quantification. To achieve this, the uncertainty quantification toolbox is utilized (42). Equations 24 and 25 denote the average calibration metric and adversarial group calibration metric, respectively.

$$P(p) = E_x[F_y(Q_{p(x)})] \; for\; all\; p \in (0,1) \tag{24}$$

$$P_{a(P)} = E_x[F_y^s(Q_{p(x)})],\; for\; all\; p \in (0,1) \\ and\; S \subseteq X\; s.t\; P(S) > 0 \tag{25}$$

where $P(p)$ represents the observed probability, E_x denotes the expectation over the input variable x, F_y is the true cumulative distribution function of the target random variable y, $Q_{p(x)}$ is the estimated pth quantile of the target random variable conditioned on x, $P_{a(P)}$ represents the observed probability under adversarial group calibration, F_y^s is the CDF of the target random variable, y, conditional on being in the subset S, and $P(S) > 0$ ensures that the subset S has a non-zero probability mass.

The average calibration metric is an essential tool for assessing a model's uncertainty. During prediction, an α-prediction interval can be established to encompass observed values within a specified α percentage of cases. By varying α and calculating the fraction of test data within this interval, one can generate a calibration plot. This plot maps the predicted proportion of test data within the interval on the x-axis against the observed proportion on the y-axis. An ideally calibrated model will align with the line f(x) = x. The misclassification area, the area between the produced curve and the f(x) = x line, can be used to define how miscalibrated the developed model is. It should be mentioned that a truly accurate model would require calibration for each unique case, but this is often impractical due to the limited data availability. Adversarial group calibration (Equation 25) involves creating multiple random subsets from the test data, calculating miscalibration for each subset, and then reporting the highest miscalibration observed. This metric is a more reliable tool to evaluate predictive uncertainty quantification in case of limited test data. The plot below shows an adversarial group calibration plot for developed models as the subset size varies along the x-axis. The process is repeated multiple times for each subset size, and the shaded area represents the standard error.

Notably, a well-calibrated model should consistently exhibit low calibration error across all group sizes. Figure 5 illustrates the mean calibration and adversarial group calibration plots for hybrid ANN-optimized models. The INFO-ANN algorithm demonstrates the lowest miscalibration value of 0.04. Furthermore, it consistently shows minimal calibration error across diverse group sizes, surpassing other models in individual calibration. In contrast, the WSO-ANN algorithm has the highest miscalibration value of 0.11, while EVO-ANN and CSA-ANN both have a miscalibration value of 0.06, ranking them second.

5. 3. Comparison with Empirical Models The predictive efficacy of the proposed INFO-ANN bond force model is critically evaluated against the forecasts derived from established analytical formulations. Specifically, comparisons are made with the bond strength models articulated by Zuo and Darwin (43) (Equation 26) and the model developed under the auspices of the Joint ACI-ASCE Committee 408 (26) (Equation 27). This comparative study seeks to ascertain the relative accuracy and applicability of the INFO-ANN model in replicating established empirical bond strength predictions, thereby providing a quantitative benchmark against conventional bond strength prediction equations widely recognized in the domain of reinforced concrete research.

In Equations 26 and 27, $t_r = 9.6R_r + 0.28$ and $t_d = 0.78d_b + 0.22$, other parameters were previously defined.

$$F_b = [((59.8l_s \cdot (C_{\min} + 0.5d_b) + 2350A_b) \cdot (0.1\frac{C_{\max}}{C_{\min}} + 0.9) + (31.14t_r t_d \frac{N_s A_t}{N_b} + 4) f_c^{0.5})] f_c^{0.25} \quad (26)$$

$$F_b = \left[(59.9 \cdot l_s \cdot (C_{\min} + 0.5d_b) + 2400A_b) \cdot (0.1\frac{C_{\max}}{C_{\min}} + 0.9) + (30.88t_r t_d \frac{N_s A_t}{N_b} + 3) \cdot f_c^{0.5} \right] \cdot f_c^{0.25} \quad (27)$$

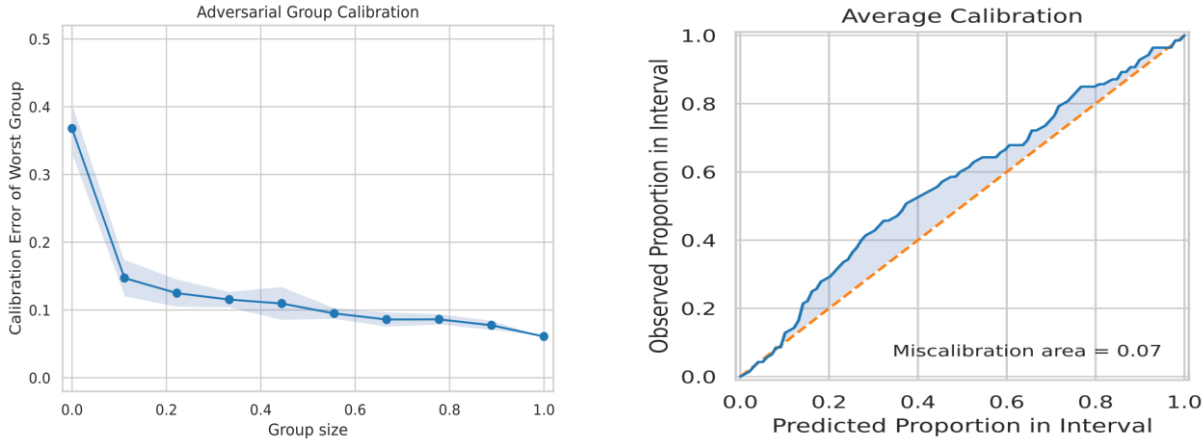

a) AEO-ANN

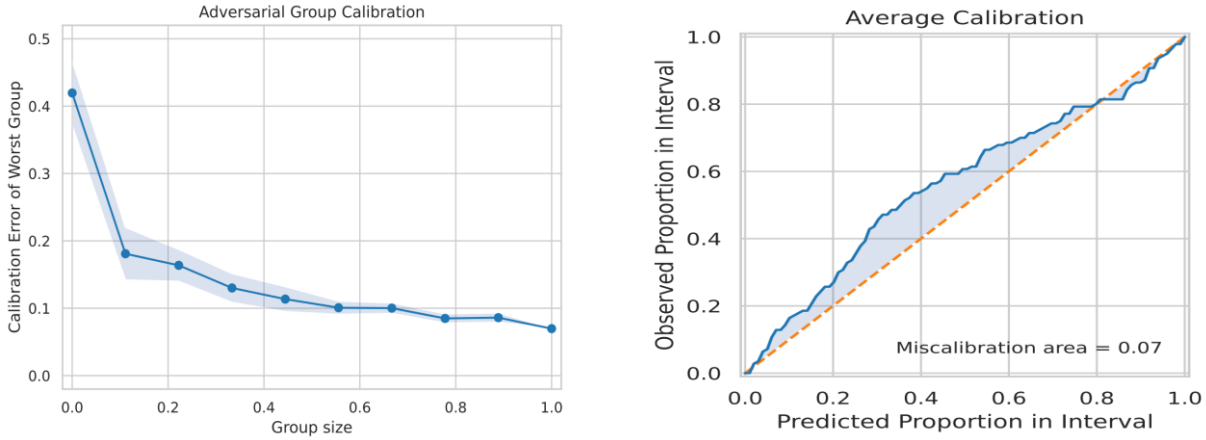

b) BBOA-ANN

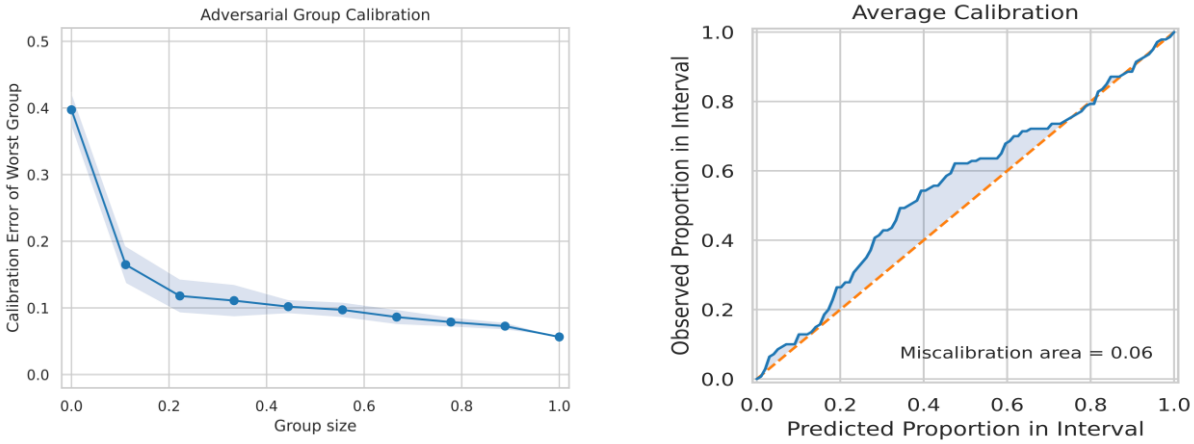

c) CSA-ANN

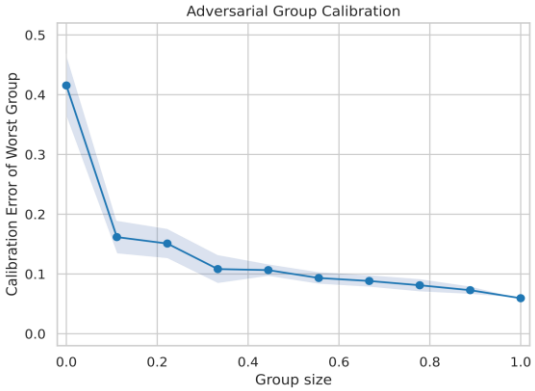

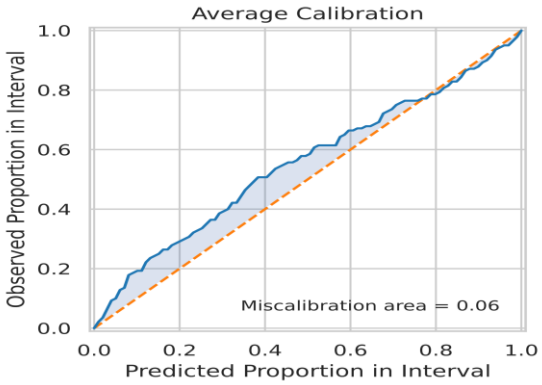

d) EVO-ANN

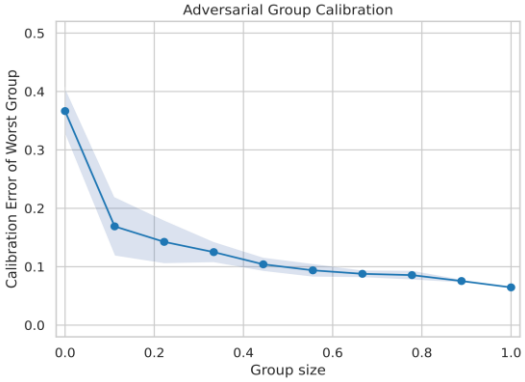

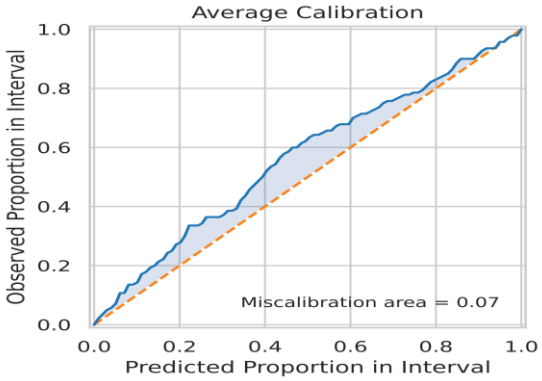

e) GWO-ANN

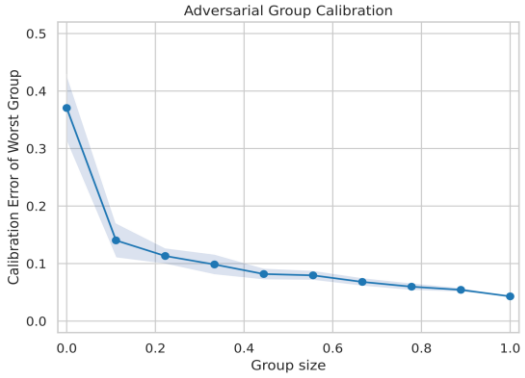

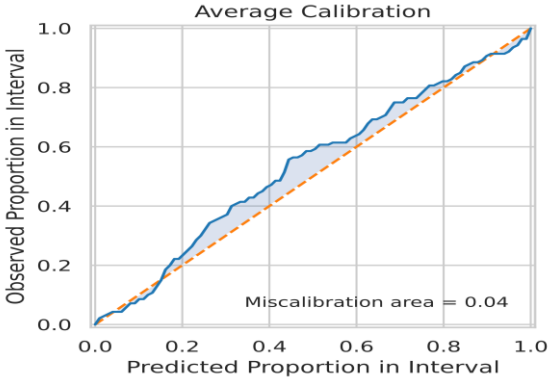

f) INFO-ANN

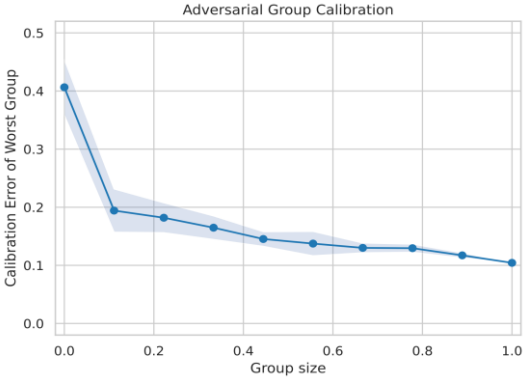

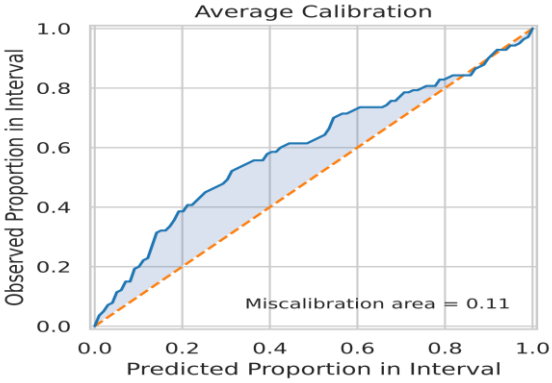

g) WSO-ANN

Figure 5. Average calibration and adversarial group calibration plot

Figures 6(a) and 6(b), respectively, show the box plot and the scatter plot of the results provided by empirical models, Equations 26 and 27. For comparison purposes, the distributions of the outputs of the proposed optimized ANN models are also depicted in these figures. The statistical performance indices for both empirical models are also presented in Table 4.

According to Table 4, the MSE for the Zuo and Darwin model (43) is 0.0083, while the ACI Committee 408 model shows an MSE of 0.0082. The R^2 value for the Zuo and Darwin model (43) is 0.880, while the ACI (26) model maintains a higher value of 0.890. This indicates that the ACI (26) model has a better capability to predict and explain the variability in the outcome variable. Comparing the performance indices in Tables 2 and 4, demonstrated that the INFO-ANN model outperforms both empirical models provided by Zuo and Darwin (43) (Equation 26) and ACI-ASCE Committee 408 (26). To assess the performance improvement of the INFO-ANN model compared to the ACI (26) model, we can calculate the percentage change for each metric. The INFO-ANN model shows a 25% improvement in MSE, indicating significantly fewer errors squared on average, suggesting better accuracy in predicting numerical outcomes compared to the ACI (26) model. The improvement in R^2 by approximately 4.38% for the INFO-ANN model indicates a stronger ability to explain the variation in the dependent variable based on the independent variables. This metric reflects a more consistent and accurate model performance compared to the ACI (26).

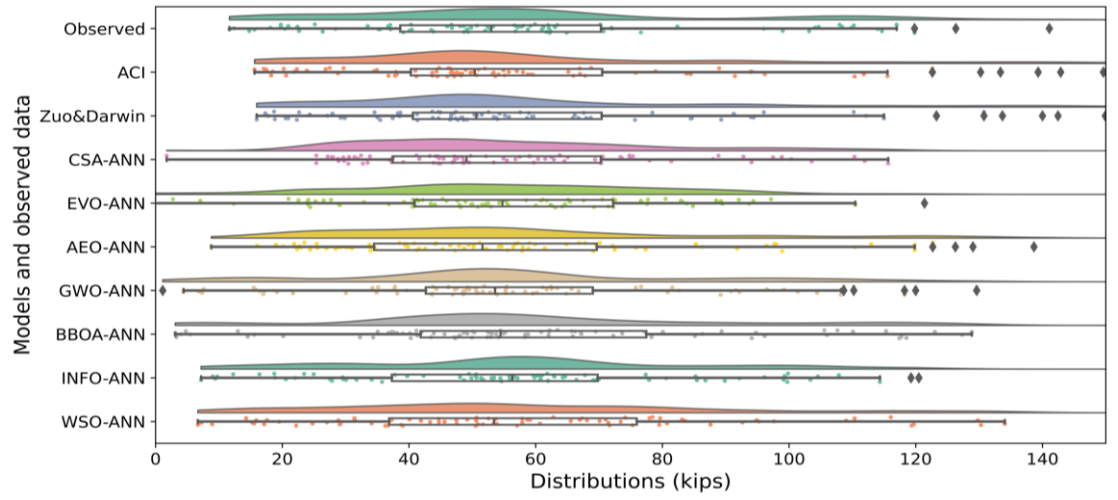

a) Distribution of the output variable

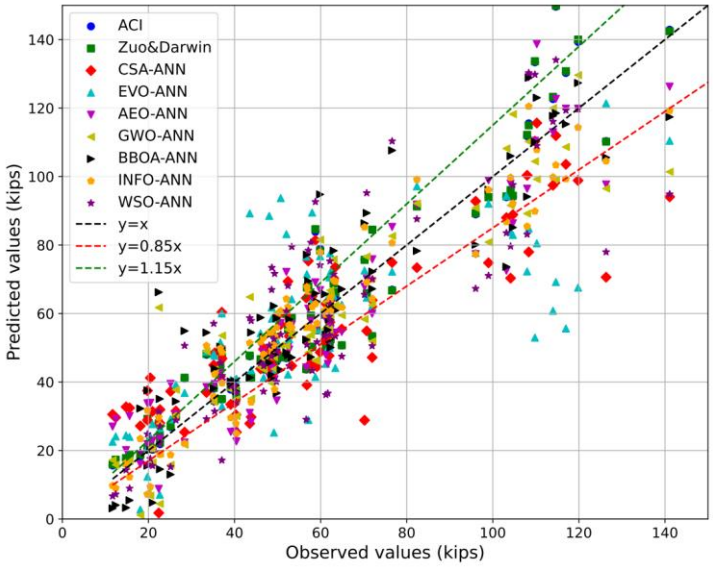

b) Scatter plot

Figure 6. Distribution of the output variable and scatter plot of the modes' results

TABLE 4. The performance of existing empirical models

Model	Performance index		
	MSE	MAE	R^2
Zuo and Darwin (43)	0.0083	0.0556	0.880
ACI Committee 408 (26)	0.0082	0.0554	0.890

5. 4. Interpreting Info-ANN Model The assessment of predictor impacts within a predictive model is a foundational pursuit spanning various domains, encompassing statistics, machine learning, and decision science (44). This evaluative undertaking entails meticulous scrutiny, validation, and refinement of the model, achieved through a comprehensive understanding of each predictor's individual influence on the prediction outcome (44). This granular understanding not only facilitates the discernment of pivotal components steering the forecasts but also enriches the model's transparency and reliability. Grounded in game theory principles, the SHAP (Shapley Additive Explanations) framework (45) presents a structured method for assessing the distinct contributions of predictors within predictive models. By conceptualizing prediction as a cooperative game wherein each predictor assumes the role of a player endeavoring to maximize their utility, the SHAP methodology assigns significance to the Shapley value associated with each predictor. This value represents the predictor's average marginal contribution across all feasible coalitions, thus quantifying its impact on shaping the prediction outcome. Essentially, the Shapley value embodies an equitable apportionment of the prediction's reward among predictors based on their collaborative efforts. SHAP explanations adhere to an additive model formulation, as expressed by the ensuing equation (45):

$$e(Vec) = SV_0 + \sum_{j=1}^{C_M} SV_j Vec \tag{28}$$

where Vec symbolizes a coalition vector that delineates the inclusion (denoted by 1) or exclusion (denoted by 0) of features within the model. The variable C_M signifies the maximum coalition size allowable within the framework. Meanwhile, SV_j denotes the SHAP values attributed to each predictor within the model. The computation of SHAP values relies on a val-function, the detailed intricacies of which are expounded by Lundberg and Lee (45). This methodological approach affords a thorough comprehension of the inner workings of the predictive model, enabling insights into the salience of individual predictors in influencing the prediction outcomes. Within this framework, the INFO-ANN model has been specifically selected for integration with SHAP functions, aiming to discern the critical components steering the forecasts.

Figure 7 exhibits the average influence of input variables on the model's output, utilizing SHAP mean values. The visual representation importance of input features within the examined framework, highlighting the cross-sectional area of the bar (A_b) as the most dominant factor, followed by the length of development or splice (l_s), the diameter of the reinforcing bar (d_b), the count of transverse reinforcements—either stirrups or ties—positioned within the specified length of development or splice (N_s), and the compressive strength of concrete (f_c).

The cross-sectional area of the bar directly influences the available surface area for adhesion between the bar and the surrounding concrete matrix. A larger cross-sectional area typically results in a greater interface for bond formation, leading to enhanced bond strength. Following the cross-sectional area of the bar, the length of development or splice holds significance in determining bond strength. A longer development or splice length allows for more extensive interaction between the bar and concrete, facilitating stronger adhesion and consequently higher bond strength. Conversely, a shorter length may restrict the bond interface, potentially reducing bond strength. The diameter of the reinforcing bar also plays a crucial role in bond strength. A larger diameter bar typically offers greater mechanical interlock with the surrounding concrete due to increased surface irregularities. This results in enhanced bond strength compared to smaller diameter bars, which may have a comparatively lower interfacial area and therefore weaker bond strength. Transverse reinforcements provide lateral confinement to the concrete cover, thereby enhancing its ability to resist splitting forces and preventing bond failure. A higher count of transverse reinforcements typically leads to

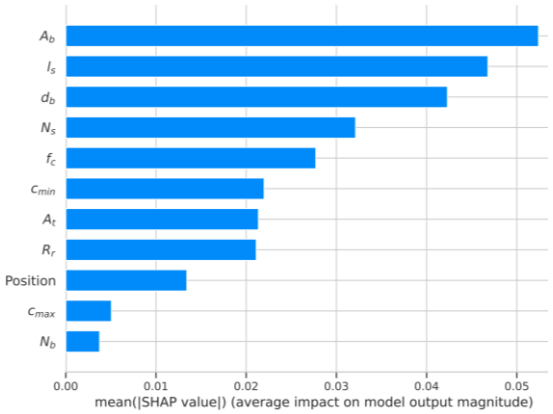

Figure 7. Average impact of input variables

improved bond strength by mitigating the risk of concrete cover spalling or delamination. Lastly, the compressive strength of concrete significantly affects bond strength. Higher concrete compressive strength generally corresponds to greater interfacial adhesion between the bar and concrete matrix, resulting in stronger bond performance. This relationship underscores the importance of ensuring adequate concrete strength to achieve desired bond strength levels in reinforced concrete structures (46-48).

Figure 8 presents a summary plot for the INFO-ANN model, where each horizontal marker on the graph illustrates how increasing values of various features influence the output, distinguishing between high impact (red) and low impact (blue) on bond strength of deformed bars in concrete. The plot indicates that increments in the cross-sectional area of the bar, the length of development or splice, the diameter of the reinforcing bar, the count of transverse reinforcements within the specified length of development or splice, the minimum/maximum concrete covers, and the compressive strength of concrete, all lead to an increase in bond strength. However, the plot also reveals that interpreting the impact of the number of reinforcing bars subjected to development or splicing becomes challenging due to the overlap of data points. This overlap may obscure distinct trends and effects directly attributable to the number of reinforcing bars, complicating clear inferences from the model output about this specific feature.

5. 5. Sobol Sensitivity Analysis (SSA) Sobol Sensitivity Analysis (SSA) (49, 50) is a potent method for evaluating how changes in a model's input parameters affect its output. The Sobol sequence is used in this technique to sample the input space more uniformly than more conventional random sampling techniques. Decomposing the outcome variance into contributions from each individual input parameter and their interactions is the main objective of SSA. Sobol indices, which measure the percentage of the output variance related to each input parameter, are used to mathematically express this. The total Sobol index S_{Ti} accounts for the contributions of all interactions involving X_i can be expressed as (49):

$$S_{Ti} = \frac{V(E[Y \mid X_{-i}])}{V[Y]} \tag{29}$$

where $V[Y]$ is the total variance of the model output Y, and $E[Y \mid X_{-i}]$ is the expected value of Y given all input parameters except X_i.

Figure 9 displays the total Sobol index of input variables on the model's output. The figure demonstrates that the importance of input features aligns well with the SHAP results. It highlights the cross-sectional area of the bar as the most significant factor. The diameter of the reinforcing bar is ranked second, and the length of development or splice is ranked third in importance. Other parameters, in order of influence, are the compressive strength of concrete and the number of transverse reinforcements—either stirrups or ties—positioned within the specified length of development or splice.

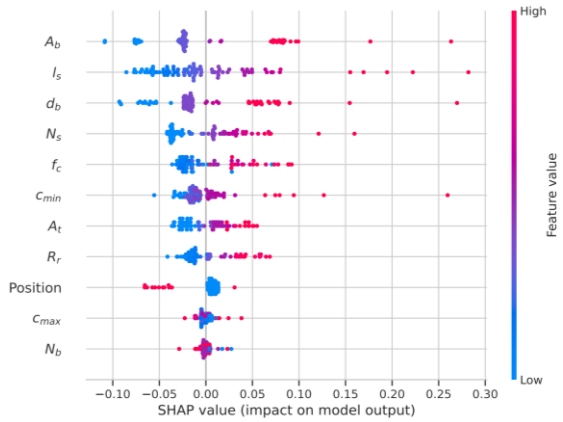

Figure 8. Summary SHAP plot for INFO-ANN model

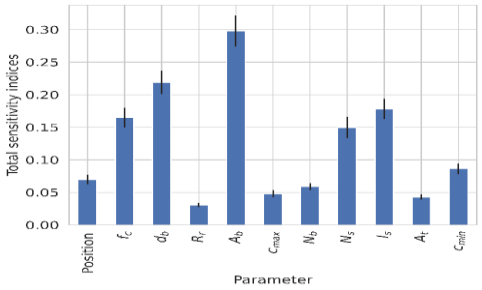

Figure 9. Sensitivity analysis plot for INFO-ANN model

6. CONCLUSION

This study delves into the critical domain of predicting bond strength between concrete and reinforcing bars, which is pivotal for ensuring the stability and longevity of reinforced concrete structures. The bond-complex structure at splice and anchorage regions holds significant importance, as it directly impacts the structural integrity of buildings, bridges, and other concrete structures. The necessity for accurate estimation of bond strength is underscored by the potential risks posed by structural weaknesses, which could compromise the safety of these structures. While previous studies have primarily relied on artificial neural networks (ANNs) for bond strength prediction, this research endeavors to advance the field by introducing a novel approach: a hybrid metaheuristic-optimized neural network model. The Grey Wolf optimizer (GWO), Energy valley optimizer (EVO), Circle search algorithm

(CSA), Artificial Ecosystem-Augmented optimization (AEO), War Strategy Optimization (WSO), and Brown-Bear optimization algorithm (BBOA) were employed to tune hyper-parameters of the ANN. Leveraging seven metaheuristic algorithms for optimization, this study seeks to enhance the precision and efficiency of bond strength predictions. Key findings include:

- Model Performance: The INFO-ANN and AEO-ANN models consistently outperformed others in both the training and testing phases. INFO-ANN, in particular, exhibited the lowest Mean Squared Error (MSE) and Mean Absolute Error (MAE) values, along with the highest R^2 scores, indicating superior predictive accuracy and model fit.
- Optimal Neural Network Configuration: The optimal number of neurons varied across models but generally fell within a specific range that balanced computational efficiency and predictive performance.
- Comparative Analysis: When compared to traditional models such as those by Zuo and Darwin and the ACI Committee 408, the INFO-ANN model showed a significant improvement in accuracy, highlighting the advantages of integrating advanced machine learning techniques in predictive modelling. Notably, the INFO-ANN model demonstrates a significant improvement in predictive accuracy, with a 25% reduction in MSE during the testing phase compared to the ACI Committee 408 model, along with a 4.38% increase in R^2, indicating enhanced explanatory power.
- Uncertainty Quantification: INFO-ANN also demonstrated the lowest miscalibration value, indicating a high level of reliability in its predictions. This is crucial for applications requiring high confidence in predictive outcomes. Moreover, the CSA and EVO showed the same performance and achieved the second rank regarding the misclassification value, while the WSO had the worst rank.
- SHAPE-based model interpretation: Average influence analysis of input variables showed that the cross-sectional area of the bar (A_b), the length of development or splice (l_s), the diameter of the reinforcing bar (d_b), the count of transverse reinforcements (N_s), compressive strength of concrete (f_c), and the minimum concrete cover ($C_{\min}$), respectively, are the most dominant factors and have a positive effect on the bond strength; while the maximum concrete cover ($C_{\max}$) and the quantity of reinforcing bars subjected to development or splicing (N_b) had the lowest impact on the model's output.

Despite the promising results of the proposed hybrid metaheuristic-optimized neural network models, there are a limitation to this study. The models primarily focus on certain input parameters such as bar diameter, compressive strength of concrete, and transverse reinforcement count, potentially overlooking other influential factors like environmental conditions or long-term durability effects that could impact bond strength. To address the limitation, future research should aim to include a more diverse range of data encompassing various environmental conditions and concrete types to enhance the robustness and applicability of the models across different scenarios. Furthermore, incorporating additional predictive variables, such as temperature variations, chemical exposure, and long-term load effects, could provide a more comprehensive understanding of factors influencing bond strength. Future studies could also explore the development of more computationally efficient models or the application of other advanced machine learning techniques, such as deep learning or ensemble methods, to improve prediction accuracy while reducing the computational load. Finally, the integration of real-time monitoring data into these predictive models could facilitate their use in ongoing structural health monitoring and maintenance, ensuring more proactive and reliable infrastructure management.

Overall, this study underscores the importance of accurate bond strength prediction in ensuring the safety and reliability of reinforced concrete structures. By introducing a novel hybrid metaheuristic-optimized neural network model and leveraging advanced interpretability techniques, this research contributes to the advancement of predictive modeling in structural engineering. Moving forward, further research can explore additional optimization techniques and incorporate a wider range of influential factors to enhance the precision and applicability of bond strength prediction models.

7. ACKNOWLEDGEMENTS

The authors would like to acknowledge the financial support of Bozorgmehr University of Qaenat for the research grant number: 39264.

8. REFERENCES

1. Adnan A, Parung H, Tjaronge M, Djamaluddin R. Bond between steel reinforcement bars and seawater concrete. Civil Engineering Journal. 2020;6:61-8. https://doi.org/10.28991/cej-2020-SP(EMCE)-06
2. Barkhordari MS, Tehranizadeh M, Scott MH. Numerical modelling strategy for predicting the response of reinforced

concrete walls using Timoshenko theory. Magazine of Concrete Research. 2021;73(19):988-1010. https://doi.org/10.1680/jmacr.19.00542

3. Cavaleri L, Barkhordari MS, Repapis CC, Armaghani DJ, Ulrikh DV, Asteris PG. Convolution-based ensemble learning algorithms to estimate the bond strength of the corroded reinforced concrete. Construction and Building Materials. 2022;359:129504. https://doi.org/10.1016/j.conbuildmat.2022.129504
4. Barkhordari M, Tehranizadeh M. Ranking passive seismic control systems by their effectiveness in reducing responses of high-Rise buildings with concrete shear walls using multiple-Criteria decision making. International Journal of Engineering. 2020;33(8):1479-90. https://doi.org/10.5829/ije.2020.33.08b.06
5. Massone LM, Rosa J, Mesa Á, editors. Versatile hysteretic model of reinforcing steel bars with buckling. Structures; 2023: Elsevier. https://doi.org/10.1016/j.istruc.2022.12.023
6. Tang C-W, Cheng C-K. Modeling local bond stress–slip relationships of reinforcing bars embedded in concrete with different strengths. Materials. 2020;13(17):3701. https://doi.org/10.3390/ma13173701
7. Degtyarev VV. Machine Learning Models for Predicting Bond Strength of Deformed Bars in Concrete. ACI Structural Journal. 2022;119(5). http://dx.doi.org/10.12989/scs.2023.49.1.109
8. Kim D-J, Kim MS, Yun GY, Lee YH. Bond strength of steel deformed rebars embedded in artificial lightweight aggregate concrete. Journal of Adhesion Science and Technology. 2013;27(5-6):490-507. https://doi.org/10.1080/01694243.2012.687552
9. Reis E, De Azevedo R, Christoforo A, Poggiali F, Bezerra A, editors. Bonding of steel bars in concrete: A systematic review of the literature. Structures; 2023: Elsevier. https://doi.org/10.1016/j.istruc.2023.01.141
10. Dancygier AN, Katz A, Wexler U. Bond between deformed reinforcement and normal and high-strength concrete with and without fibers. Materials and Structures. 2010;43:839-56. https://doi.org/10.1617/s11527-009-9551-6
11. Shirgaonkar AA, Patil YD. Experimental and Analytical Study on the Longitudinal Shear Bond Behaviour of Basalt Textile-Reinforced Concrete Composite Slab. Journal of Rehabilitation in Civil Engineering. 2023;11(4):91-121. https://doi.org/10.22075/jrce.2023.27455.1664
12. Habibi SA, Hemmati A, Naderpour H. An Innovative Approach to Estimate Chloride Diffusion Coefficient in Submerged Concrete Structures Using Soft Computing. Journal of Rehabilitation in Civil Engineering. 2023;11(3):88-106. https://doi.org/10.22075/jrce.2022.28128.1697 https://civiljournal.semnan.ac.ir/article_7194_3931493ff90d07594ebbcbfe69e5cbf6.pdf
13. Khansar HH, Chafjiri AS, Fathollahi-Fard AM, Gheibi M, Moezzi R, Parsa J, et al. Meta-Heuristic-Based Machine Learning Techniques for Soil Stress Prediction in Embankment Dams During Construction. Indian Geotechnical Journal. 2024:1-23. https://doi.org/10.1007/s40098-024-01032-2
14. Tsang L, Ghorbani A, Khatami SMH, Ulrikh DV. Intelligent Classification of Stable and Unstable Slope Conditions Based on Landslide Movement. Journal of Rehabilitation in Civil Engineering. 2024;12(3):17-31. https://doi.org/10.22075/jrce.2023.30293.1833 https://civiljournal.semnan.ac.ir/article_8159_52f8cc422ff472583e17bad15156cf2e.pdf
15. Gholizadeh H, Fathollahi-Fard AM, Fazlollahtabar H, Charles V. Fuzzy data-driven scenario-based robust data envelopment analysis for prediction and optimisation of an electrical discharge machine's parameters. Expert Systems with Applications. 2022;193:116419. https://doi.org/10.1016/j.eswa.2021.116419
16. Pizarro PN, Massone LM. Structural design of reinforced concrete buildings based on deep neural networks. Engineering Structures. 2021;241:112377. https://doi.org/10.1016/j.engstruct.2021.112377
17. Mousapour Mamoudan M, Ostadi A, Pourkhodabakhsh N, Fathollahi-Fard AM, Soleimani F. Hybrid neural network-based metaheuristics for prediction of financial markets: a case study on global gold market. Journal of computational design and engineering. 2023;10(3):1110-25. https://doi.org/10.1093/jcde/qwad039
18. Li M, Qi J, Tian X, Guo H, Liu L, Fathollahi-Fard AM, et al. Smartphone-based straw incorporation: An improved convolutional neural network. Computers and Electronics in Agriculture. 2024;221:109010. https://doi.org/10.1016/j.compag.2024.109010
19. Dahou Z, Sbartaï ZM, Castel A, Ghomari F. Artificial neural network model for steel–concrete bond prediction. Engineering Structures. 2009;31(8):1724-33. https://doi.org/10.1016/j.engstruct.2009.02.010
20. Nguyen T-H, Nguyen T, Truong TT, Doan DTV, Tran D-H, editors. Corrosion effect on bond behavior between rebar and concrete using Bayesian regularized feed-forward neural network. Structures; 2023: Elsevier. https://doi.org/10.1016/j.istruc.2023.03.128
21. Golafshani EM, Rahai A, Sebt MH, Akbarpour H. Prediction of bond strength of spliced steel bars in concrete using artificial neural network and fuzzy logic. Construction and building materials. 2012;36:411-8. https://doi.org/10.1016/j.conbuildmat.2012.04.046
22. Rinchon JPM, Concha NC, Calilung MGV, editors. Reinforced concrete ultimate bond strength model using hybrid neural network-genetic algorithm. 2017IEEE 9th International Conference on Humanoid, Nanotechnology, Information Technology, Communication and Control, Environment and Management (HNICEM); 2017: IEEE. https://doi.org/10.1109/HNICEM.2017.8269560
23. Huang T, Liu T, Xu N, Yue K, Li Y, Liu X, et al. A data-driven approach for predicting interface bond strength between corroded reinforcement and concrete. Structures. 2023;57:105122. https://doi.org/10.1016/j.istruc.2023.105122
24. Ahmad MS, Adnan SM, Zaidi S, Bhargava P. A novel support vector regression (SVR) model for the prediction of splice strength of the unconfined beam specimens. Construction and building materials. 2020;248:118475. https://doi.org/10.1016/j.conbuildmat.2020.118475
25. Degtyarev VV. Artificial Neural Network to Predict Bond Strength of Deformed Bars in Concrete. Special Publication. 2021;350:81-9. https://doi.org/10.14359/51734314
26. Committee A. Bond and development of straight reinforcing bars in tension (ACI 408R-03). American Concrete Institute, Detroit, Michigan, US. 2003;49.
27. Soledispa CE, Pizarro PN, Massone LM. Optimizing reinforced concrete walls and columns through artificial neural networks with structural neighbor-based features. Journal of Building Engineering. 2024:109223. https://doi.org/10.1016/j.jobe.2024.109223
28. Safaeian Hamzehkolaei N, MiarNaeimi F. A new hybrid multi-level cross-entropy-based moth-flame optimization algorithm. Soft Computing. 2021;25(22):14245-79. https://doi.org/10.1007/s00500-021-06109-1
29. Hamzehkolaei NS, Kadkhoda N. An efficient ranked Voronoi diagram-based hybrid method for reliability-based structural analysis and design optimization. Soft Computing. 2023;27(19):13889-910. https://doi.org/10.1007/s00500-023-08450-z https://doi.org/10.1007/s00500-023-08450-z

30. Pradeep T, GuhaRay A, Bardhan A, Samui P, Kumar S, Armaghani DJ. Reliability and prediction of embedment depth of sheet pile walls using hybrid ANN with optimization techniques. Arabian Journal for Science and Engineering. 2022;47(10):12853-71. https://doi.org/10.1007/s13369-022-06607-w
31. Zhang G, Hamzehkolaei NS, Rashnoozadeh H, Band SS, Mosavi A. Reliability assessment of compressive and splitting tensile strength prediction of roller compacted concrete pavement: introducing MARS-GOA-MCS. International Journal of Pavement Engineering. 2022;23(14):5030-47. https://doi.org/10.1080/10298436.2021.1990920
32. Ashrafian A, Hamzehkolaei NS, Dwijendra NKA, Yazdani M. An evolutionary neuro-fuzzy-based approach to estimate the compressive strength of eco-friendly concrete containing recycled construction wastes. Buildings. 2022;12(8):1280. https://doi.org/10.3390/buildings12081280
33. Mirjalili S, Mirjalili SM, Lewis A. Grey wolf optimizer. Advances in engineering software. 2014;69:46-61. https://doi.org/10.1016/j.advengsoft.2013.12.007
34. Azizi M, Aickelin U, A. Khorshidi H, Baghalzadeh Shishehgarkhaneh M. Energy valley optimizer: a novel metaheuristic algorithm for global and engineering optimization. Scientific Reports. 2023;13(1):226. https://doi.org/10.1038/s41598-022-27344-y
35. Qais MH, Hasanien HM, Turky RA, Alghuwainem S, Tostado-Véliz M, Jurado F. Circle search algorithm: A geometry-based metaheuristic optimization algorithm. Mathematics. 2022;10(10):1626. https://doi.org/10.3390/math10101626
36. Ahmadianfar I, Heidari AA, Noshadian S, Chen H, Gandomi AH. INFO: An efficient optimization algorithm based on weighted mean of vectors. Expert Systems with Applications. 2022;195:116516. https://doi.org/10.1016/j.eswa.2022.116516
37. Menesy AS, Sultan HM, Korashy A, Banakhr FA, Ashmawy MG, Kamel S. Effective parameter extraction of different polymer electrolyte membrane fuel cell stack models using a modified artificial ecosystem optimization algorithm. Ieee Access. 2020;8:31892-909. https://doi.org/10.1109/ACCESS.2020.2973351
38. Ayyarao TS, Ramakrishna N, Elavarasan RM, Polumahanthi N, Rambabu M, Saini G, et al. War strategy optimization algorithm: a new effective metaheuristic algorithm for global optimization. IEEE Access. 2022;10:25073-105. https://doi.org/10.1109/ACCESS.2022.3153493
39. Prakash T, Singh PP, Singh VP, Singh SN. A novel Brown-bear optimization algorithm for solving economic dispatch problem. Advanced Control & Optimization Paradigms for Energy System Operation and Management: River Publishers; 2023. p. 137-64.
40. Malozyomov BV, Martyushev NV, Babyr NV, Pogrebnoy AV, Efremenkov EA, Valuev DV, et al. Modelling of Reliability Indicators of a Mining Plant. Mathematics (2227-7390). 2024;12(18). 10.3390/math12182842
41. Vatani A, Jafari-Asl J, Ohadi S, Safaeian Hamzehkolaei N, Afzali Ahmadabadi S, Correia JA, editors. An efficient surrogate model for reliability analysis of the marine structure piles. Proceedings of the Institution of Civil Engineers-Maritime Engineering; 2023: Emerald Publishing Limited. https://doi.org/10.1680/jmaen.2022.020
42. Tennøe S, Halnes G, Einevoll GT. Uncertainpy: A Python Toolbox for Uncertainty Quantification and Sensitivity Analysis in Computational Neuroscience. Frontiers in Neuroinformatics. 2018;12. https://doi.org/10.3389/fninf.2018.00049 https://www.frontiersin.org/articles/10.3389/fninf.2018.00049
43. Zuo J, Darwin D, editors. Splice strength of conventional and high relative rib area bars in normal and high-strength concrete2000: American Concrete Institute.
44. Barkhordari MS, Jawdhari A. Machine learning based prediction model for plastic hinge length calculation of reinforced concrete structural walls. Advances in Structural Engineering. 2023;26(9):1714-34. https://doi.org/10.1177/13694332231174252
45. Lundberg SM, Lee S-I. A unified approach to interpreting model predictions. Advances in neural information processing systems. 2017;30.
46. Darwin D, Graham EK. Effect of deformation height and spacing on bond strength of reinforcing bars. University of Kansas Center for Research, Inc.; 1993.
47. Morris GJ. Experimental evaluation of local bond behaviour of deformed reinforcing bars in concrete structures. 2015.
48. Ogura N, Bolander JE, Ichinose T. Analysis of bond splitting failure of deformed bars within structural concrete. Engineering Structures. 2008;30(2):428-35. https://doi.org/10.1016/j.engstruct.2007.04.004
49. Saltelli A, Annoni P, Azzini I, Campolongo F, Ratto M, Tarantola S. Variance based sensitivity analysis of model output. Design and estimator for the total sensitivity index. Computer physics communications. 2010;181(2):259-70. https://doi.org/10.1016/j.cpc.2009.09.018
50. Abdollahi A, Li D, Deng J, Amini A. An explainable artificial-intelligence-aided safety factor prediction of road embankments. Engineering Applications of Artificial Intelligence. 2024;136:108854. https://doi.org/10.1016/j.engappai.2024.108854

COPYRIGHTS
©2025 The author(s). This is an open access article distributed under the terms of the Creative Commons Attribution (CC BY 4.0), which permits unrestricted use, distribution, and reproduction in any medium, as long as the original authors and source are cited. No permission is required from the authors or the publishers.

Persian Abstract

چکیده

برآورد دقیق مقاومت چسبندگی بین بتن و میلگردهای تغییر شکل یافته برای پایداری سازه‌های بتن مسلح، به ویژه در مناطق بحرانی که تحت بارهای سنگین و تنش‌های محیطی قرار دارند، ضروری است. علی‌رغم تحقیقات تجربی گسترده که پیچیدگی عوامل مؤثر بر مقاومت چسبندگی را آشکار کرده‌اند، مدل‌های پیش‌بینی موجود که اغلب به شبکه‌های عصبی مصنوعی (ANNs) متکی هستند، به دلیل مجموعه داده‌های محدود و نمایندگی ناکافی از میدان‌های تنش واقعی، دارای دقت کافی نمی‌باشند. در پاسخ به این مسئله، این مطالعه یک مدل نوآورانه شبکه عصبی بهینه‌سازی شده با الگوریتم‌های فراابتکاری ترکیبی را معرفی می‌کند که به سرعت و با دقت بالا مقاومت چسبندگی تحت بار کششی را پیش‌بینی می‌کند. با استفاده از یک مجموعه داده جامع شامل 558 نتیجه آزمایشگاهی معتبر، هفت الگوریتم فراابتکاری شامل روش میانگین وزنی بردارها (INFO)، بهینه‌ساز گرگ خاکستری (GWO)، بهینه‌ساز دره انرژی (EVO)، الگوریتم جستجوی دایره‌ای(CSA) ، بهینه‌سازی تقویت‌شده اکوسیستم مصنوعی (AEO)، بهینه‌سازی استراتژی جنگ (WSO) و الگوریتم بهینه‌سازی خرس قهوه‌ای (BBOA) برای بهینه‌سازی شبکه استفاده شد. نتایج نشان می‌دهند که مدل‌های ترکیبی توسعه یافته، به ویژه روش میانگین وزنی بردارها، عملکرد بهتری دارند. الگوریتم INFO و پس از آن CSA و EVO کمترین مقدار عدم تطابق را نشان دادند، که بیان‌گر سطح بالایی از اطمینان است. علاوه بر این، مقایسه با روابط تجربی رایج، بهبود قابل توجه عملکرد مدل پیشنهادی را نشان داد که به کاهش 25 درصدی MSE در مرحله آزمون منجر شد. همچنین، بررسی نتایج تحلیل حساسیت به همراه روش SHAP برای تفسیر مدل پیش‌بینی، نشان داد که متغیرهای سطح مقطع میلگرد، طول گسترش (اتصال)، قطر میلگرد تقویت‌کننده و مقاومت فشاری بتن پیش‌بینی‌کننده‌های کلیدی مدل می‌باشند.